

AD-A 114 962

**TECHNICAL  
LIBRARY**

AD

AD-E400 814

**TECHNICAL REPORT ARPAD-TR-81006**

**PROFILES OF CRACKS IN BASES OF 155-MM M483A1,  
M692, AND M731 PROJECTILES**

**HENRY HARTMANN**

**APRIL 1982**



**US ARMY ARMAMENT RESEARCH AND DEVELOPMENT COMMAND  
PRODUCT ASSURANCE DIRECTORATE  
DOVER, NEW JERSEY**

**APPROVED FOR PUBLIC RELEASE; DISTRIBUTION UNLIMITED.**

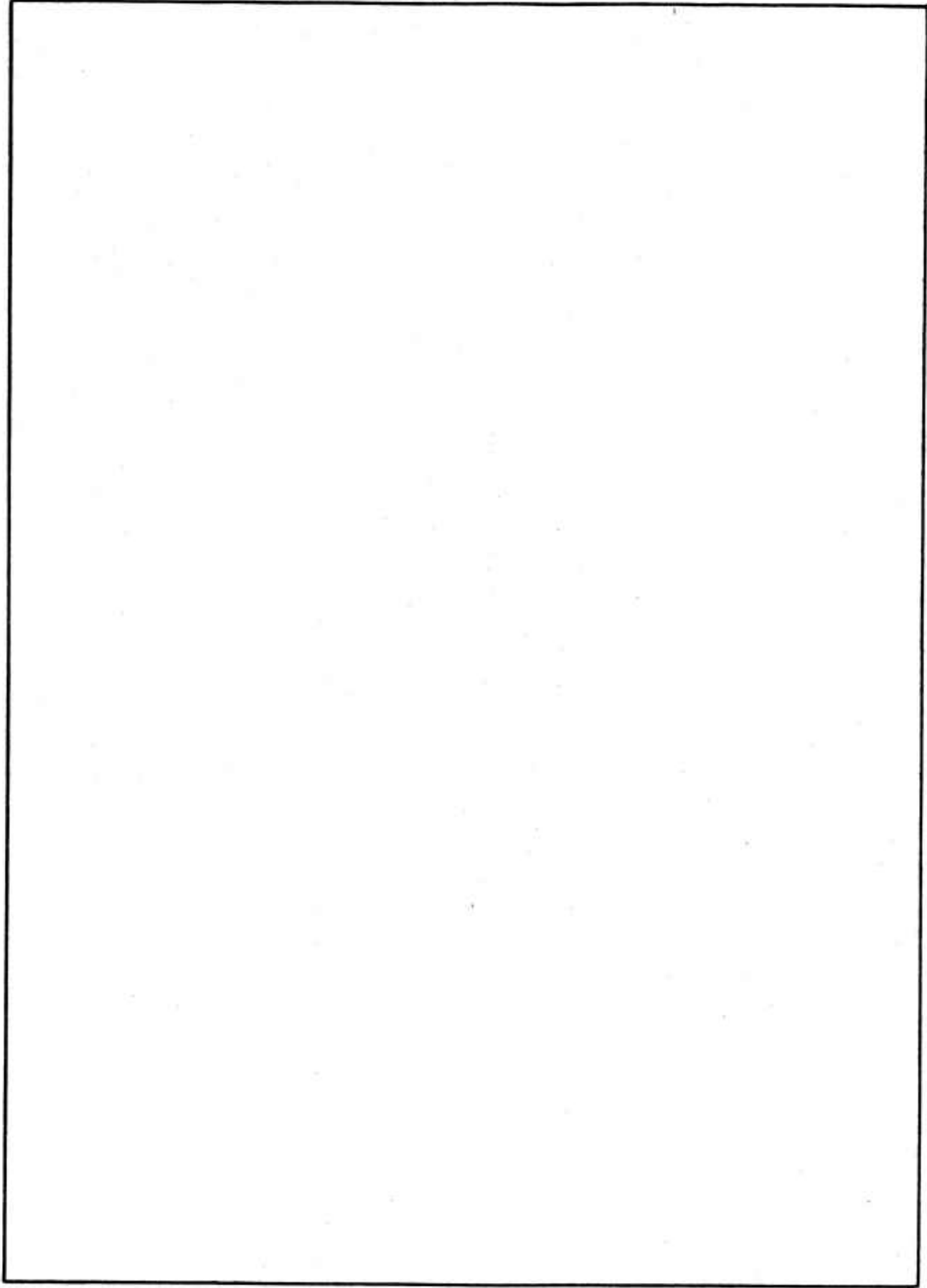
The views, opinions, and/or findings contained in this report are those of the author(s) and should not be construed as an official Department of the Army position, policy or decision, unless so designated by other documentation.

The citation in this report of the names of commercial firms or commercially available products or services does not constitute official endorsement by or approval of the U.S. Government.

Destroy this report when no longer needed. Do not return to the originator.

REPORT DOCUMENTATION PAGE		READ INSTRUCTIONS BEFORE COMPLETING FORM
1. REPORT NUMBER Technical Report ARPAD-TR-81006	2. GOVT ACCESSION NO.	3. RECIPIENT'S CATALOG NUMBER
4. TITLE (and Subtitle) PROFILES OF CRACKS IN BASES OF 155-mm M483A1, M692, AND M731 PROJECTILES	5. TYPE OF REPORT & PERIOD COVERED Final Sep 1981 - Dec 1981	
	6. PERFORMING ORG. REPORT NUMBER	
7. AUTHOR(s) Henry Hartmann	8. CONTRACT OR GRANT NUMBER(s)	
9. PERFORMING ORGANIZATION NAME AND ADDRESS ARRADCOM, PAD Technology & Automation, Information and Mathematics Div (DRDAR-QAS-T) Dover, NJ 07801	10. PROGRAM ELEMENT, PROJECT, TASK AREA & WORK UNIT NUMBERS	
11. CONTROLLING OFFICE NAME AND ADDRESS ARRADCOM, TSD STINFO Div (DRDAR-TSS) Dover, NJ 07801	12. REPORT DATE April 1982	
	13. NUMBER OF PAGES 75	
14. MONITORING AGENCY NAME & ADDRESS (if different from Controlling Office)	15. SECURITY CLASS. (of this report) Unclassified	
	15a. DECLASSIFICATION/DOWNGRADING SCHEDULE	
16. DISTRIBUTION STATEMENT (of this Report) Approved for public release; distribution unlimited.		
17. DISTRIBUTION STATEMENT (of the abstract entered in Block 20, if different from Report)		
18. SUPPLEMENTARY NOTES		
19. KEY WORDS (Continue on reverse side if necessary and identify by block number) Artillery ammunition                      Ultrasonic inspection Base    155-mm projectiles Cracks Eddy current inspection Projectiles		
20. ABSTRACT (Continue on reverse side if necessary and identify by block number)  This report shows size, shape, depth, distribution, and orientation of cracks revealed in the forward surface of 36 rejected projectile bases. These bases had been intended for use on 155-mm M483A1, M692, and M731 projectiles.		

SECURITY CLASSIFICATION OF THIS PAGE(When Data Entered)



SECURITY CLASSIFICATION OF THIS PAGE(When Data Entered)

## CONTENTS

	Page
Introduction	1
Investigation	1
Ultrasonic Inspection	1
Eddy Current Inspection	2
Fluorescent Liquid Penetrant Inspection	4
Comparison of Ultrasonic and Eddy Current Inspection Results	4
Conclusions	5
Recommendations	6
Distribution	65

## TABLES

1 Results of eddy current inspection, at 500 kHz frequency, of bases for M483A1 projectiles	7
2 Results of eddy current inspection, at 75 kHz frequency, of bases for M483A1, M692, and M731 projectiles	8
3 Fluorescent liquid penetrant inspection of bases for M483A1, M692, and M731 projectiles	13

## FIGURES

	Page
1 Base for 155-mm M483A1 projectile--forward surface	15
2 Base for 155-mm M483A1 projectile--rear surface	16
3 Ultrasonic C-scan setup	17
4 Ultrasonic sensitivity of 5 MHz shear waves in M483A1 bases	18
5 Ultrasonic clarity of 5 MHz shear waves in M483A1 bases	19
6 Ultrasonic C-scan of M483A1 base CMC/CMC 7	20
7 Ultrasonic C-scan of M483A1 base CMC/CMC 8	21
8 Ultrasonic C-scan of M483A1 base CMC/CMC 9	22
9 Ultrasonic C-scan of M483A1 base CMC/CMC 10	23
10 Ultrasonic C-scan of M483A1 base CMC/KAAP 57	24
11 Ultrasonic C-scan of M483A1 base CMC/KAAP 61	25
12 Ultrasonic C-scan of M483A1 base CMC/KAAP 62	26
13 Ultrasonic C-scan of M483A1 base CMC/KAAP 63	27
14 Ultrasonic C-scan of M483A1 base CMC/KAAP 64	28
15 Ultrasonic C-scan of M483A1 base CMC/KAAP 65	29
16 Ultrasonic C-scan of M483A1 base CMC/KAAP 66	30
17 Ultrasonic C-scan of M483A1 base CMC/KAAP 68	31
18 Ultrasonic C-scan of M483A1 base CMC/KAAP 70	32
19 Ultrasonic C-scan of M483A1 base CMC/KAAP 71	33
20 Ultrasonic C-scan of M483A1 base CMC/KAAP 75	34
21 Ultrasonic C-scan of M483A1 base CMC/KAAP 76	35
22 Ultrasonic C-scan of M483A1 base CMC/KAAP 125	36
23 Ultrasonic C-scan of M483A1 base CMC/LSAAP 296	37
24 Ultrasonic C-scan of M483A1 base CMC/LSAAP 303	38

25	Ultrasonic C-scan of M483A1 base CMC/LSAAP 305	39
26	Ultrasonic C-scan of M483A1 base CMC/LSAAP 306	40
27	Ultrasonic C-scan of M483A1 base CMC/LSAAP 307	41
28	Ultrasonic C-scan of M483A1 base CMC/LSAAP 308	42
29	Ultrasonic C-scan of M483A1 base CMC/LSAAP 309	43
30	Ultrasonic C-scan of M483 base (standard)	44
31	Eddy current standard with a variable-depth (inclined) slot in an M483A1 base	45
32	Vector dot trace for various depths of slots in the eddy current standard	46
33	Profile of crack in M692/M731 base A-CMC/LAAP 3	47
34	Profile of crack in M483A1 base CMC/LSAAP 296	48
35	Profile of crack in M692/M731 base A-CMC/LAAP 4	49
36	Profile of crack in M483A1 base CMC/KAAP 71	50
37	Profiles of cracks viewed from outside of M483A1 base CMC/LSAAP 308	51
38	Distribution of cracks in forward surface of M483A1 base CMC/KAAP 61	52
39	Location and depth of spots on M483A1 base CMC/KAAP 62	53
40	Location and depth of a spot on M483A1 base CMC/KAAP 64	54
41	Location and depth of a spot on M483A1 base CMC/KAAP 75	55
42	Location and depth of spots on M483A1 base CMC/KAAP 76	56
43	Depth of spots in forward surface of M483A1 base CMC/LSAAP 305	57
44	Fluorescent liquid penetrant indications on M692/M731 base A-CMC/KAAP 3	58
45	Fluorescent liquid penetrant indications on M483A1 base CMC/KAAP 61	59
46	Fluorescent liquid penetrant indications on M483A1 base CMC/KAAP 71	60
47	Fluorescent liquid penetrant indications on M483A1 base CMC/LSAAP 296	61
48	Fluorescent liquid penetrant indications on M483A1 base CMC/KAAP 76	62
49	Depth of spots in forward surface of M483A1 base CMC/KAAP 63	63

## INTRODUCTION

This report reveals the orientation and depth of many cracks that were found nondestructively in 155-mm M483A1 projectile bases (fig. 1). A total of 63 suspect M483A1 projectile bases were reinspected. As the investigation progressed, two cracked bases for M692 and M731 projectiles were included.

In the past it has been difficult to determine the depth of cracks in metal parts without destroying the parts. An early technique had been to cut apart an item containing a crack; to meticulously sand, polish, and optically examine the crack; and then to record the depth of the crack. This process had to be repeated over and over until the crack was consumed completely. Only in this way could the profile of a crack's depth be measured.

Recently, a technique was developed to split a brittle item along its crack. The separation revealed the whole crack. Careful machining was required to make the item separate along its crack.

Nondestructive techniques are now available. By the methods discussed in this report, the depths of cracks can be measured by both ultrasonic and eddy current inspections. Major advantages of these inspections are: (1) measurements are made faster, (2) the item is preserved for future testing, and (3) natural cracks of known size can be used for checking the accuracy of production inspection.

During the investigation, very localized flaws (called "spots") were also discovered.

## INVESTIGATION

### Ultrasonic Inspection

Ultrasonic inspection was done within a water tank which is part of a laboratory scanner. Bases were positioned under water in the center of a turntable. The forward surface of each base (fig. 1) was facing up. This position trapped air inside the rear cavity within the boattail. Care was taken to prevent any splashing inside the rear cavity (fig. 2) while each base was being placed on the turntable (fig. 3). Any droplets of water on the rear face of a base could cause false defect signals.

All of the metal within the web between front and rear surfaces was inspected. Prior investigation had revealed that a 39-degree ultrasonic shear wave inside the metal base (7075-T6 aluminum) provided the greatest sensitivity for detection of both man-made shallow slots and hemispheres. This same shear wave also produced the greatest signal-to-noise ratio (clarity). These optimum values of sensitivity and clarity are revealed in figures 4 and 5.



An S-80 Reflectoscope ultrasonic flaw detector was used to obtain data. Ultrasonic C-scans were made at a gain setting that barely revealed the presence of a 1.59 mm (0.063 in.) diameter hemisphere in the forward surface of the base. A base from an M483 projectile was used as the standard and contained five different sized hemispherical holes, plus two slots, all on the forward surface. (M483 bases are identical to M483A1 bases except the M483 has a longer boattail.) All seven targets had been mechanically cut (drilled and sawed) into the aluminum surface and were covered with waterproof tape. Calibrations with the standard were made at the beginning and end of each day to check the detection sensitivity of the inspection process. Since the standard stood taller, the ultrasonic transducer had to be raised during each calibration to maintain a constant water path.

The immersion-type ultrasonic transducer had a 6.4 mm (0.25 in.) diameter active element with a flat lens. It produced a 5.0-MHz peak frequency broadband pulse.

Ultrasonic C-scans were made of all bases. Most of the C-scans which showed flaws (figs. 6 through 29) are included in this report. All detected flaws were on the forward surface of the bases. The gain setting for the ultrasonic flaw detector was 50 decibels. A sample calibration using the standard is shown in figure 30.

## Eddy Current Inspection

### Process

The eddy current inspection process was accomplished on a metal turning lathe. Each base was mounted on a headstock and rotated, first with one face outward and then the other, so that both forward and rear faces were inspected. An EM-3300 flaw detector was used at a frequency setting of 500 kHz. A standard flat surface probe (44B022-4) was used. The probe is rated for use at a frequency range of 400 kHz to 1 MHz. A base from an M483A1 projectile was used as a standard. This standard contained two slots in the rear surface. One slot was 0.18 mm (0.007 in.) deep, and the other was 0.30 mm (0.012 in.) deep. These slots were used to calibrate the inspection process. The cathode ray tube screen on the flaw detector was set to register a 1-cm-high signal when a 0.18-mm-deep slot was detected.

After all 63 M483A1 projectile bases were inspected (table 1), nine of these bases were selected for a more thorough analysis. In addition, two bases for M692 and M731 projectiles from prior work were also included. At the time this work was done, the minimum critical crack had been designated as being 3.73 mm (0.147 in.) deep. The depth of flaws in the 11 chosen bases was as close as available to that of the minimum critical crack.

Four different eddy current probes were tried with the same flaw detector on a variable-depth (inclined) slot standard (fig. 31). The goal was to obtain optimum discrimination within a slot depth range of 0 to 6.3 mm (0 to 0.25

in.). Frequencies between 2 and 500 kHz were tried. The eddy current probe with the lowest frequency (2 kHz) gave weak response to slot signals. Its large face hampered accurate location, and it could not detect the presence of shallow slots. The best combination was a 50-to-400 kHz probe, no. A144B022-3, which was used at a frequency of 75 kHz. When used on the EM-3300 Multitester, this combination produced good discrimination for various depths of slots (fig. 32).

Lightly drawn lines, often 2.5 mm (0.10 in.) apart, were made in a parallel-line pattern on the surface of the bases. The lines were oriented to cross the cracks at approximate right angles. These lines provided intersections with the cracks at which eddy current readings were taken. Black felt-tip pen marks were used to amplify the position of the cracks. The depth along the inclined slot in the standard which gave a matching reading was recorded as the depth of the crack. Direction of measurement along cracks was clockwise on the circular surface of each base (table 2).

#### Limitations of Accuracy

Eddy current measurements had some limitations. Measurements for cracks deeper than 0.30 mm (0.012 in.) were extrapolated (table 1). This extrapolation creates error because the relationship between signal amplitude and depth-of-crack is not linear. Because of this error in eddy current extrapolation, ultrasonic C-scans were used to designate deep cracks.

#### Measurement of Depth Profile of Cracks

From the 12 bases selected for further analysis, six were found to have cracks. Four of the six bases with single cracks are shown in figures 33 through 36. The illustrated profiles are depth portraits of cracks as they would appear if the cracks were on a flat plane. Single cracks that exceed the minimum critical depth are illustrated in figures 33 and 34. However, the cracks are well removed from the center of the bases. Whether these are actually critical cracks is not known now. The other two smaller cracks shown in figures 35 and 36 are not critical. Two bases had multiple cracks (figs. 37 and 38). An example of a profuse distribution of cracks is shown in figure 38.

#### Measurement of Spots

From the 12 bases selected for further analysis, six were found to have spots. Spots are considered to be inclusions or porosity-type-defects. The distribution of some of the spots is illustrated in figures 39 through 42. The difference in eddy current sensitivity between the use of 500-kHz and 75-kHz frequencies is illustrated in figure 42. The three spots shown, which were originally detected with the more sensitive 500-kHz probe, are just barely perceptible with the 75 kHz probe. Another difference in eddy current sensitivity is illustrated in figure 43. The deepest spot that was originally measured as being

greater than 5 mm with 500 kHz eddy current frequency, is measured as 1.8 mm deep with 75 kHz frequency.

Spot size is determined by one reading denoted as "depth." However, substantial error can exist in the measurement. Error comes from the difference in shape between spot-type defects and the slots that are used to calibrate the equipment. Also, the distance beneath the surface where the spot begins contributes to the error.

#### Fluorescent Liquid Penetrant Inspection

Eleven bases were inspected with fluorescent liquid penetrant (table 3). Five of these bases were known to have cracks. Four revealed their cracks (figs. 44 through 47). Base no. A-CMC/LAAP 4 did not reveal its crack. It was later found with eddy current inspection (table 2) that this crack was small, having a length of 10 mm (0.4 in.) and a maximum depth of 0.6 mm (0.02 in.). The other six bases had spots. Only three of these spots (all in base no. CMC/KAAP 76) were revealed by fluorescent liquid penetrant (fig. 48). This occurrence hints that the spots in the other five bases were beneath the surface.

The flaws revealed by fluorescent liquid penetrant were recorded by marking over the indications with a black felt-tip pen. The same pen was used with eddy current inspection to outline the other flaws that were not revealed by fluorescent liquid penetrant.

#### Comparison of Ultrasonic and Eddy Current Inspection Results

##### General Findings

Data from both ultrasonic and eddy current inspection processes are listed in table 1. Out of a total of 63 suspect M483A1 projectile bases that were inspected, 34 bases were found to contain flaws. About half of the flaws were cracks. The remaining flaws were spots. All cracks were found to occur on the forward surface. However, spots occurred on both surfaces.

##### Sensitivity

Sensitivity is defined as the smallest depth of flaw that can be reliably detected. Eddy current inspection proved to be more sensitive than ultrasonic inspection. Shown below are the depths of cracks and spots detected by ultrasonic and eddy current inspections.

<u>Inspection</u>	<u>Depth (mm)</u>	
	<u>Crack</u>	<u>Spot</u>
Ultrasonic (only deepest portions of cracks and spots were recorded)	1.5	0.6
Eddy current:		
500 kHz (only deepest portions of cracks and spots were recorded)	1.5	0.18
75 kHz (all portions of cracks and spots were recorded)	0.10	0.10

The sensitivity of 75 kHz eddy current for detecting both crack and spot depths is 0.10 mm (0.004 in.). The limit of sensitivity for both 500 kHz eddy current and ultrasonic inspections was not reached. However, the ultrasonic sensitivity to detect spots should be close to 0.6 mm (0.02 in.) because three out of four 0.3 mm deep spots were not detected.

If a flaw is oriented parallel to the direction of scan of an eddy current probe (or parallel to the direction of ultrasound), its presence will be more difficult to detect. For example, in base CMC/KAAP 63 (fig. 13), eddy current inspection failed to detect a spot that had been picked up by ultrasonics. The base was reexamined by spinning it in a lathe and carefully moving the eddy current probe across the forward surface. No flaw signal occurred. This procedure was repeated many times with no sign of any flaw. Then, with figure 13 used as a guide, the area containing the spot was located. Moving the eddy current probe through the located area in a radial direction revealed the spot. However, moving the probe in a circumferential direction across the spot (as occurred during regular eddy current inspection) failed to reveal its presence. The spot is listed as 0.40 mm (0.016 in.) deep (fig. 49). An adjacent spot is barely perceptible with eddy current. This base had been rejected by eddy current at Kansas Army Ammunition Plant.

## CONCLUSIONS

For the limited sample size inspected, the following conclusions are drawn:

1. Two types of defects are encountered in bases: cracks and spots. The spots are small in size. They occur in both forward and rear surfaces. Some spots are at surface level while others are below.

2. About half of the flawed bases have spots. Eddy current measurements indicate depths of spots as shallow as 0.10 mm (0.004 in.). This depth is the limit of sensitivity for 75 kHz eddy current inspection.

3. Cracks are generally much deeper than spots. The shallowest crack encountered is 0.6 mm (0.024 in.) deep. Most of the cracks exceed a depth of 5 mm (0.20 in.).

4. All cracks are in the forward surface of the bases.

#### RECOMMENDATIONS

1. A study should be made to determine whether spots are crucial defects. This study can be done through destructive analysis of a significant sample size of spots. If spots are determined not to be crucial, the induced magnetic field of the probe can be enlarged to reduce its sensitivity to small spots. Savings can be made by acceptance of small spots.

2. It is recommended that all 18 M483A1 bases with critical size cracks be subjected to a hydrotest-to-failure, which simulates firing stresses. Such a test would reveal data about the critical crack size, as well as the strength of cracked bases.

Table 1. Results of eddy current inspection, at 500 kHz frequency<sup>a</sup>, of bases for M483A1 projectiles

(mfr/rec'd from)	Base Serial no.)	Type		Discontinuity Indication			Maximum depth (mm)	Discontinuity confirmed by ultrasonic inspection	History
		Crack	Spot	Location	On forward surface	On rear surface			
CMC/CMC	7	X					>5	X	(b)
CMC	8	X					>5	X	
CMC	9	X					>5	X	
CMC	10	X					>5	X	
KAAP	57	X					>5	X	
KAAP	59	X	X				>5	X	
KAAP	61	X					0.3	X	
KAAP	62	X	X				>5	X	
KAAP	63	X	X				0.9	X	
KAAP	64	X	X				0.6 <sup>d</sup>	X	
KAAP	65	X	X				1.25	X	
KAAP	66	X	X				>5	X	
KAAP	68	X	X				>5	X	
KAAP	70	X	X				>5	X	
KAAP	71	X					>5	X	
KAAP	74	X	X				1.3	X	
KAAP	75	X	X				0.3	X	
KAAP	76	X	X				0.6	X	
LSAAP	125	X	X				0.3	X	
KAAP	142	X	X				>5	X	
LSAAP	296	X	X				>5	X	
LSAAP	303	X	X				>5	X	
LSAAP	305	X	X				>5	X	
LSAAP	306	X	X				>5	X	
LSAAP	307	X	X				>5	X	
LSAAP	308	X	X				>5	X	
LSAAP	309	X	X				>5	X	
NOR/KAAP	323	X	X				0.18	X	
KAAP	324	X	X			X	0.3	X	
KAAP	325	X	X			X	0.18	X	
KAAP	326	X	X			X	0.18	X	
KAAP	327	X	X			X	0.3	X	
CMC/LSAAP	330	X	X			X	0.18	X	
NOR/NOR	360	X	X			X	0.18	X	

<sup>a</sup> Equipment used: EM-3300 multitester with 400 kHz - 1 MHz probe no. 44B022-4.

<sup>b</sup> Visual rejects at Chamberlain Corporation.

<sup>c</sup> Eddy current indications revealed at Kansas Army Ammunition Plant; from group of 27.

<sup>d</sup> Not detected initially by circular scan.

<sup>e</sup> Eddy current indications revealed at Lone Star Army Ammunition Plant; from group of 24.

<sup>f</sup> Eddy current indications revealed at Lone Star Army Ammunition Plant; from group of 17.

<sup>g</sup> Eddy current indications revealed at Kansas Army Ammunition Plant for indications on rear surface.

<sup>h</sup> Eddy current indications revealed at Lone Star Army Ammunition Plant; from group of 13.

<sup>i</sup> Eddy current indications revealed at Norris Corporation.

Table 2. Results of eddy current inspection, at 75 kHz frequency<sup>a</sup>, of bases for M483A1, M692, and M731 projectiles

<u>Base<sup>b</sup></u> <u>(mfr/rec'd from serial no.)</u>	<u>No.</u>	<u>Type</u>		<u>Distance along crack (mm)</u>	<u>Depth (mm)</u>	<u>Maximum depth<sup>c</sup> (mm)</u>
		<u>Crack</u>	<u>Spot</u>			
A-CMC/LAAP	3		X	0	0.1	
				3	0.4	
				5	1.3	
				8	1.3	
				10	1.3	
				13	1.4	
				15	1.5	
				18	1.5	
				20	1.5	
				23	3.8	
				25	3.8	
				28	3.8	
				30	5.0	
				33	5.0	
				35	5.0	
				38	5.0	
				40	5.0	
				43	2.5	
				45	2.5	
				48	2.5	
				50	2.5	
				53	0.6	
				55	0.6	
				58	0.6	
				60	0.6	
				63	0.6	

<sup>a</sup> Equipment used: EM-3300 multitester with 50- to 400-kHz probe All4B022-3.

<sup>b</sup> First two listed bases (with prefix A) are used on M692 and M731 projectiles; remaining bases are used on M483A1 projectiles.

<sup>c</sup> Values for spots have limited accuracy.

Table 2. (cont)

<u>Base<sup>b</sup></u> <u>(mfr/rec'd from serial no.)</u>	<u>No.</u>	<u>Type</u>		<u>Distance</u> <u>along</u> <u>crack (mm)</u>	<u>Depth (mm)</u>	<u>Maximum</u> <u>depth<sup>c</sup></u> <u>(mm)</u>
		<u>Crack</u>	<u>Spot</u>			
A-CMC/LAAP	4	X		0	0.1	
				3	0.1	
				5	0.4	
				8	0.6	
				10	0.6	
CMC/KAAP	61	X				2.5
		X				5.8
		X				>6.0
		X				>6.0
		X				>6.0
		X				3.8
		X				5.0
		X				>6.0
		X				>6.0
		X				5.8
		X				>6.0
		X				>6.0
		X				>6.0
		X				>6.0
CMC/KAAP	62		X			0.6
			X			0.4
CMC/KAAP	63		X			0.1
			X			0.4
CMC/KAAP	64		X			1.3
CMC/KAAP	71	X				
				3	0.5	
				5	0.6	
				8	1.3	
				10	1.3	
				13	0.6	



Table 2. (cont)

<u>(mfr/rec'd from serial no.)</u>	Base b	No.	Type		Distance along crack (mm)	Depth (mm)	Maximum depth <sup>c</sup> (mm)
			Crack	Spot			
CMC/KAAP	75	-		X			0.4
CMC/KAAP	76	1	X				0.1
		2	X				0.1
		3	X				0.1
CMC/LSAAP	296	-	X		3	5.8	
					6	5.5	
					9	5.3	
					12	5.3	
					15	5.3	
					18	5.3	
					22	2.5	
					25	0.8	
CM/LSAAP	305	1		X			0.3
		2		X			0.1
		3		X			0.5
		4		X			1.8
		5		X			0.6
		6		X			0.4
		7		X			0.9
		8		X			0.4
		9		X			0.8
		10		X			0.3
		11		X			0.5
CMC/LSAAP	308	1	X		2	1.9	
					8	1.5	
					16	1.5	
					22	1.9	
					26	1.3	
					32	1.9	
					41	1.3	
					50	0.8	

Table 2. (cont)

CMC/LSAAP	Base <sup>b</sup> (mfr/rec'd from serial no.)	No.	Type		Distance along crack (mm)	Depth (mm)	Maximum depth <sup>c</sup> (mm)
			Crack	Spot			
308		2	X		2	1.9	0.5
					6	2.3	
		3	X		9	2.2	
					14	2.3	
					18	1.9	
					2	0.8	
					5	2.0	
					11	2.0	
					19	2.0	
		4			25	1.3	
					30	0.9	
					40	0.9	
					47	2.0	
					56	1.8	
					64	0.6	
5				2	1.3		
				8	0.1		
				16	0.1		
				25	1.0		
				28	2.3		
				32	2.0		
				38	1.8		
				43	1.3		
				47	0.6		
				52	0.4		
6			X	1	0.9		
				4	1.8		
				8	1.8		
				11	1.8		
				17	2.3		
				23	1.9		
				27	1.9		
				32	1.3		
36	1.3						

Table 2. (cont)

<u>Base<sup>b</sup></u> <u>(mfr/rec'd from serial no.)</u>	<u>No.</u>	<u>Type</u>		<u>Distance along crack (mm)</u>	<u>Depth (mm)</u>	<u>Maximum depth<sup>c</sup> (mm)</u>
		<u>Crack</u>	<u>Spot</u>			
CMC/LSAAP	7			1	1.8	
				6	2.0	
				13	2.0	
				18	2.0	
				26	1.8	
				31	2.3	
				39	2.3	
	8	X		45	2.5	
				6	2.3	
				9	2.3	
				16	0.4	

Table 3. Fluorescent liquid penetrant inspection of bases for M483A1, M692, and M731 projectiles

<u>Base*</u> <u>(mfr/rec'd from serial no.)</u>		<u>Discontinuity</u> <u>indications</u> <u>on forward</u> <u>surface</u>	<u>Remarks</u>
A-CMC/LAAP	3	X	Crack
A-CMC/LAAP	4		
CMC/KAAP	61	X	Cracks (spider-type) extending beyond undercut of threads of shoulder
CMC/KAAP	62		
CMC/KAAP	63		
CMC/KAAP	64		
CMC/KAAP	71	X	Crack
CMC/KAAP	75		
CMC/KAAP	76	X	Three spots
CMC/LSAAP	296	X	Crack
CMC/LSAAP	305		

---

\* First two listed bases (with prefix A) are used on M692 and M731 projectiles; remaining bases are used on M483A1 projectiles.



Figure 1. Base for 155-mm M483A1 projectile--forward surface



Figure 2. Base for 155-mm M483A1 projectile--rear surface

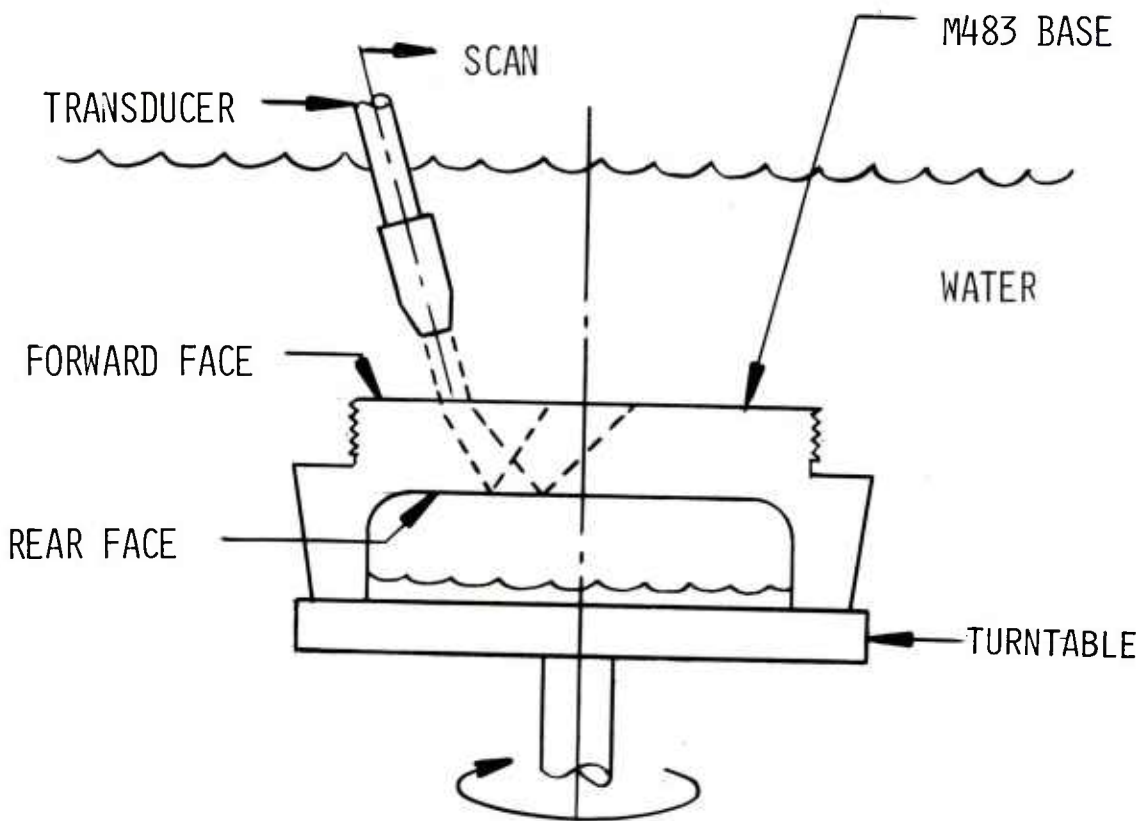


Figure 3. Ultrasonic C-scan setup

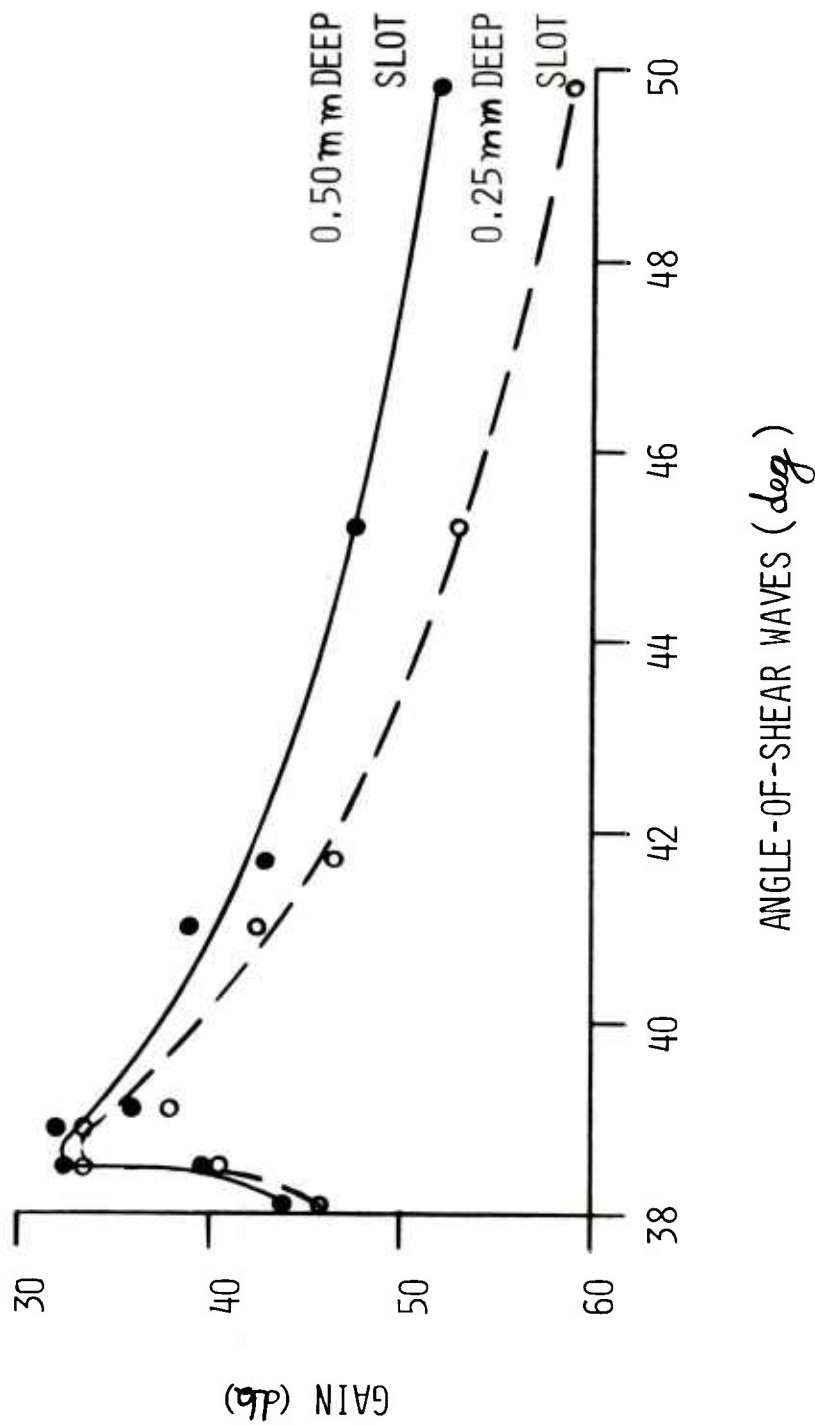


Figure 4. Ultrasonic sensitivity of 5 MHz shear waves in M483Al bases



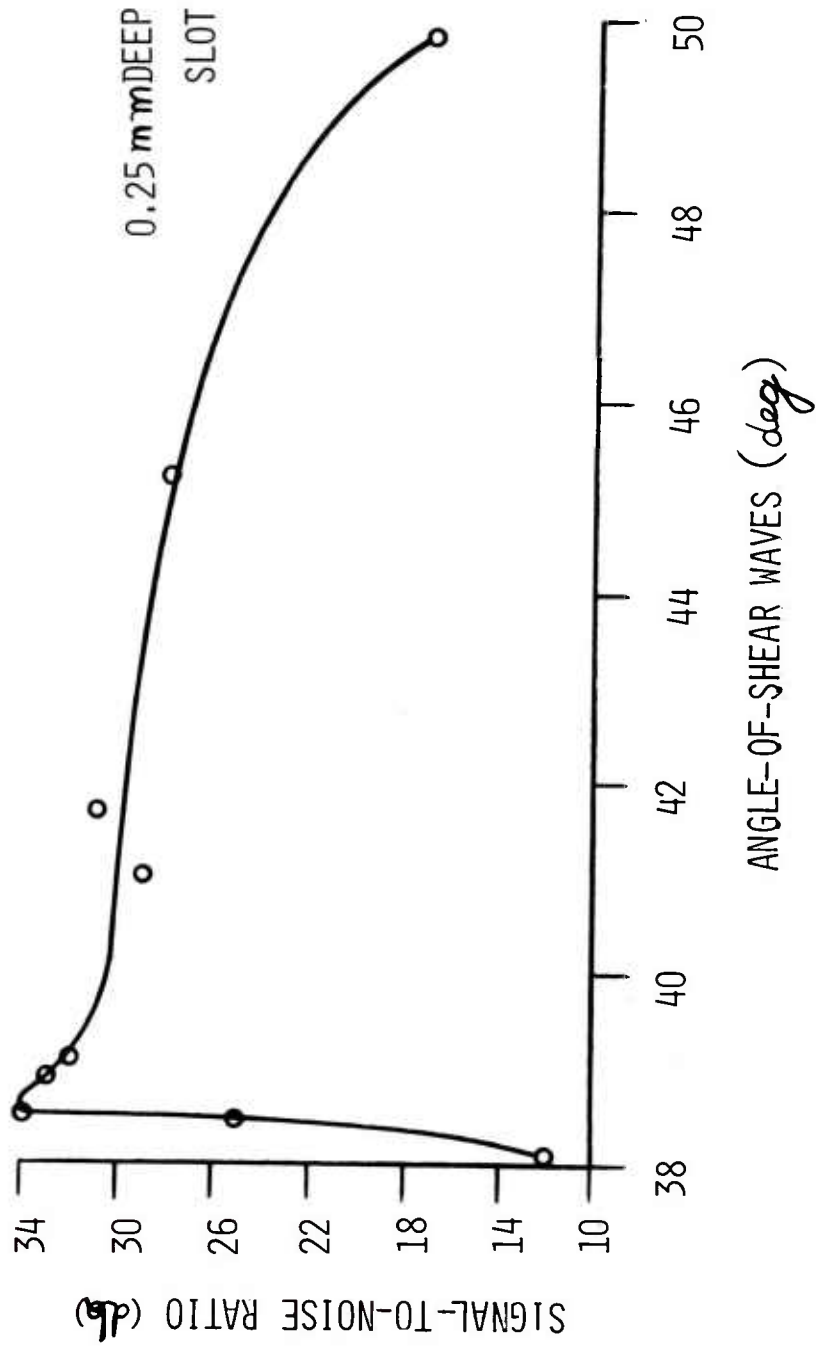


Figure 5. Ultrasonic clarity of 5 MHz shear waves in M483A1 bases

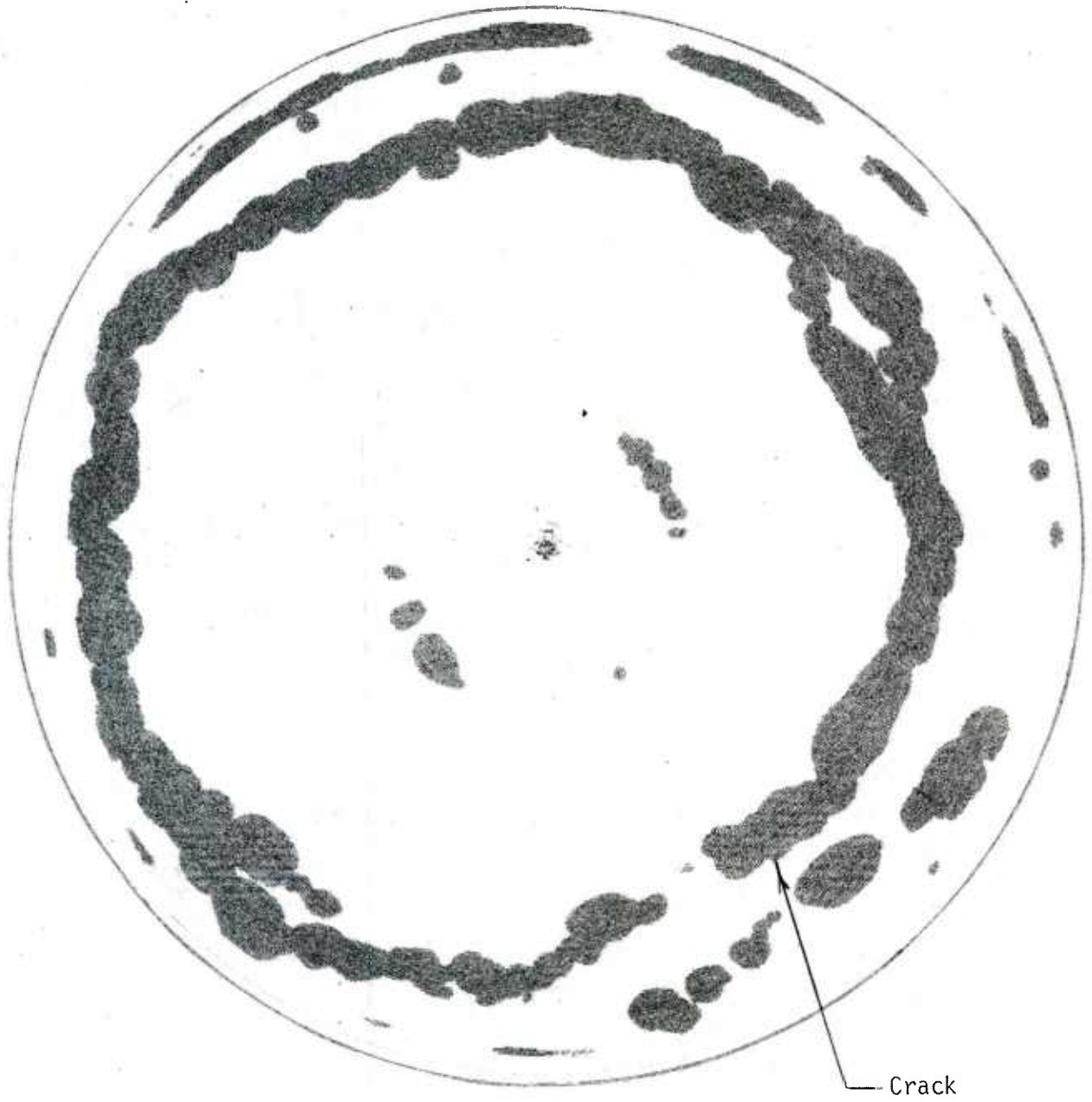


Figure 6. Ultrasonic C-scan of M483A1 base CMC/CMC 7

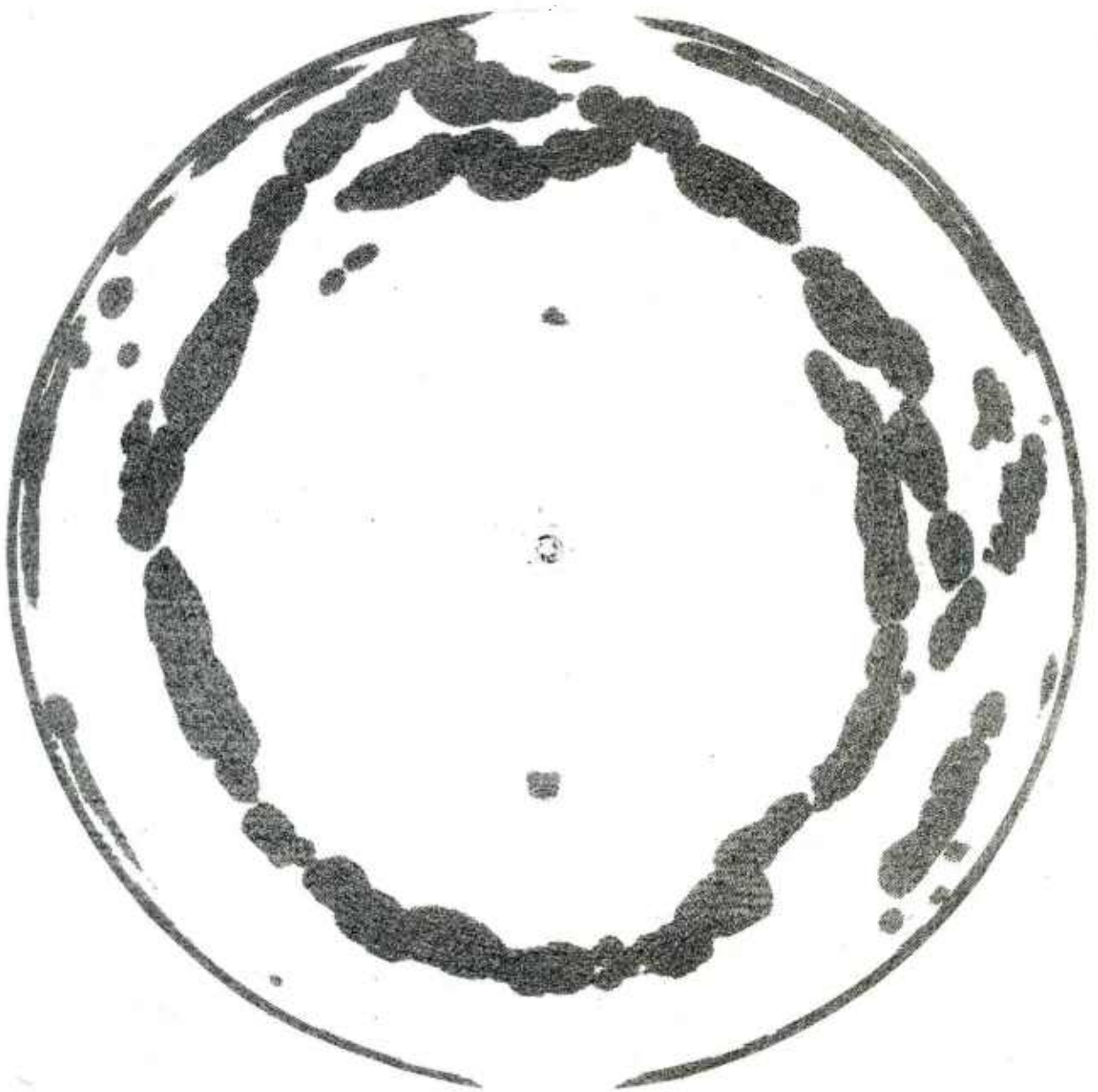


Figure 7. Ultrasonic C-scan of M483A1 base CMC/CMC 8

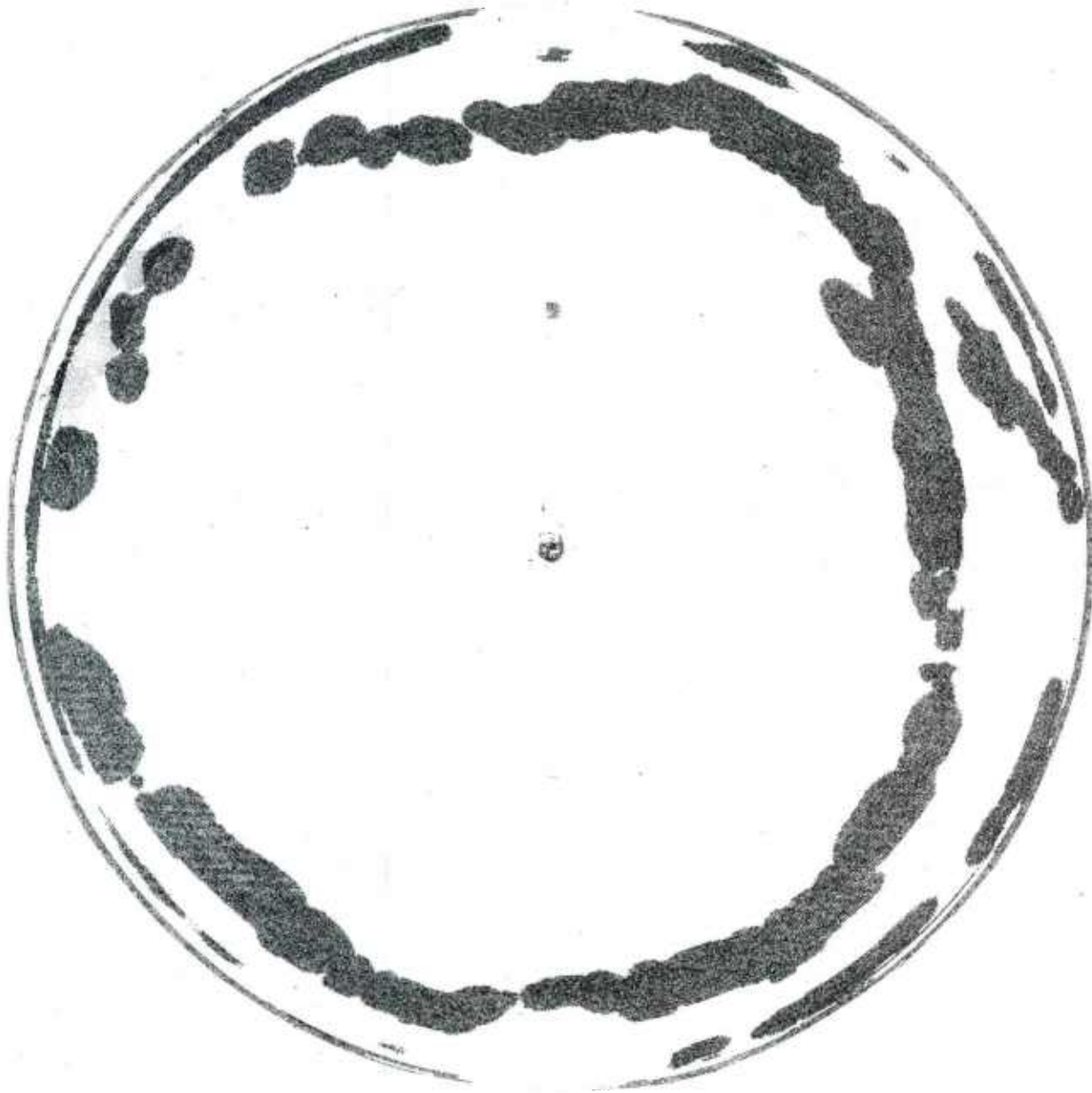


Figure 8. Ultrasonic C-scan of M483A1 base CMC/CMC 9

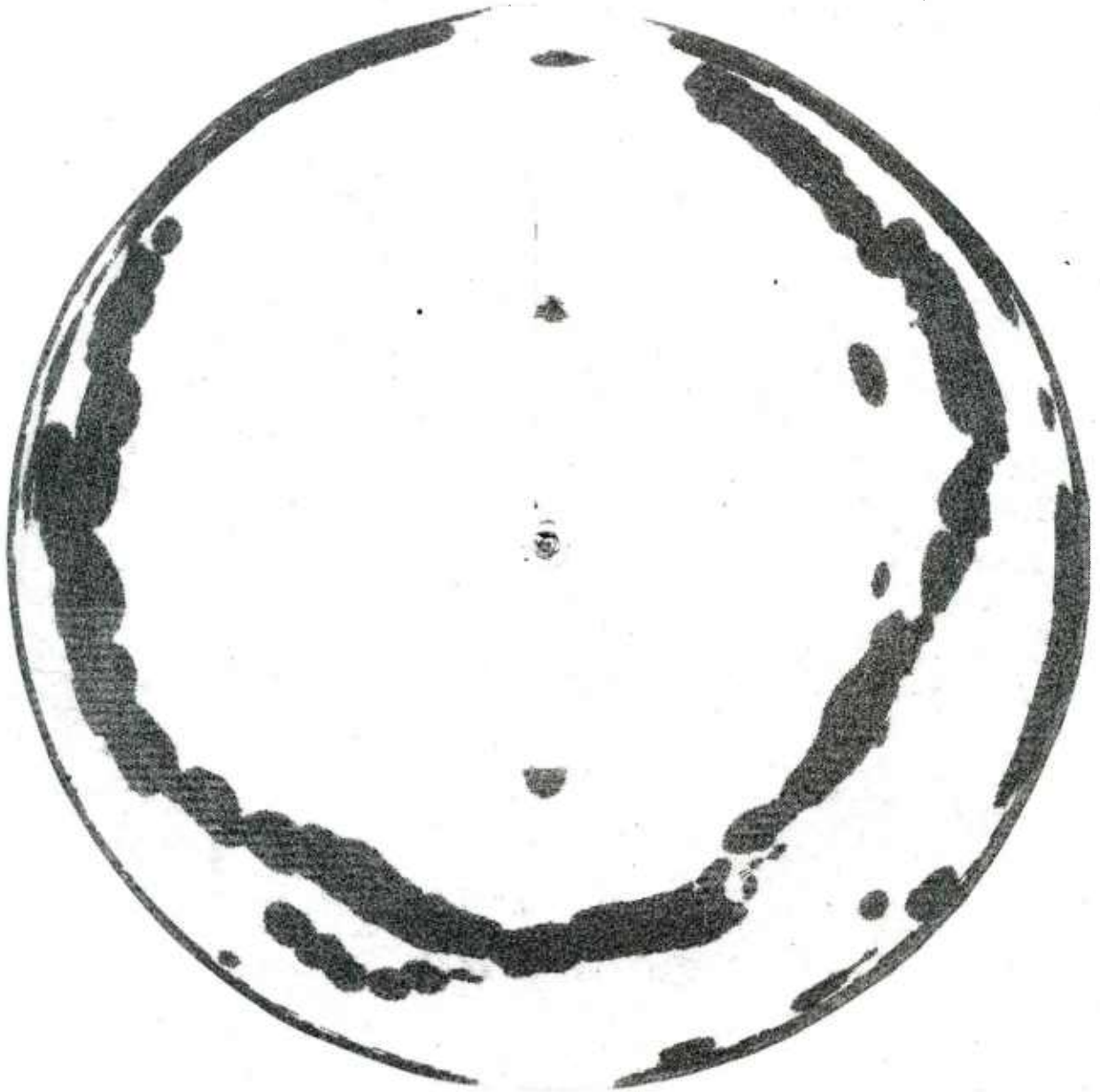


Figure 9. Ultrasonic C-scan of M483A1 base CMC/CMC 10

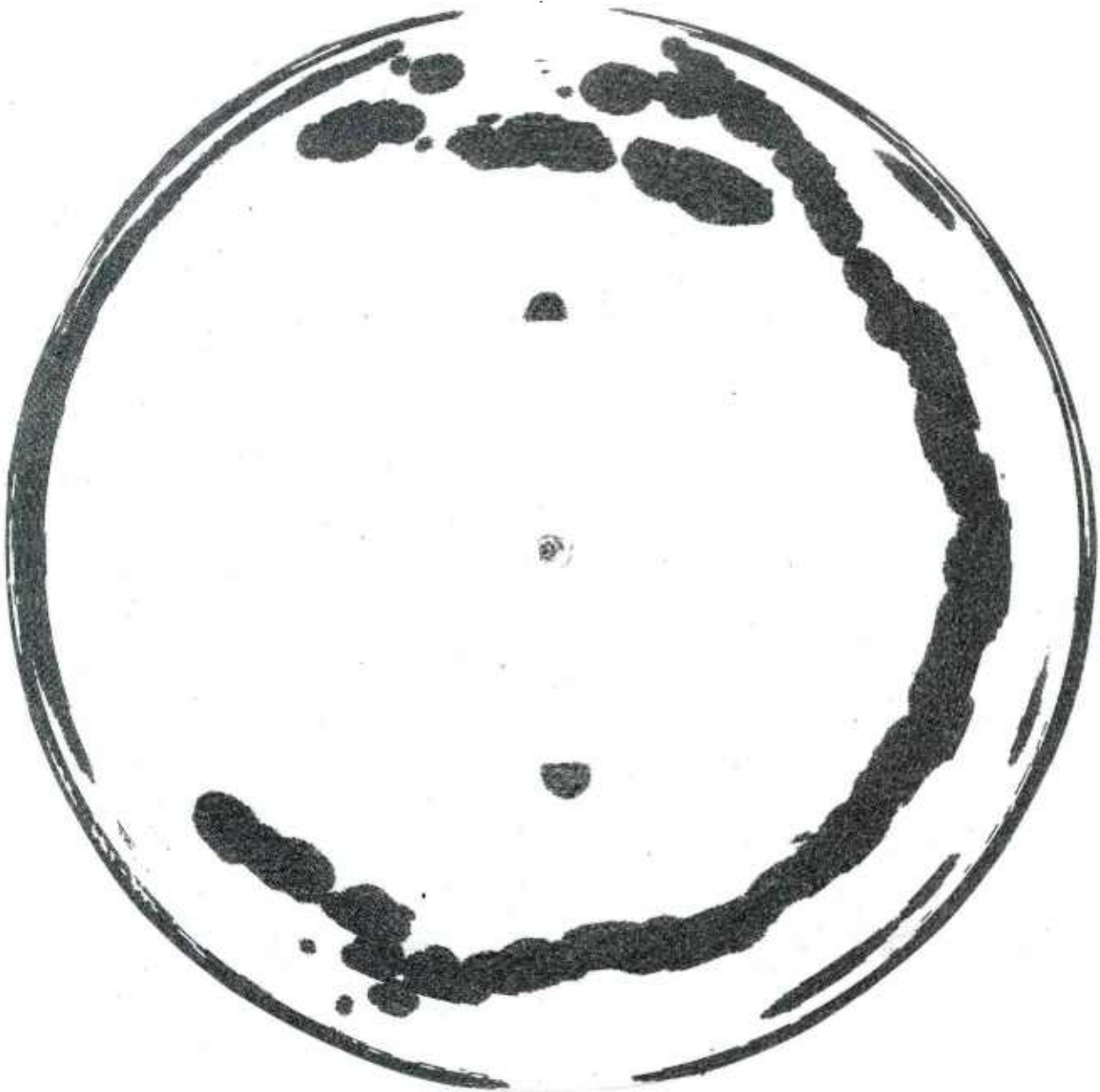


Figure 10. Ultrasonic C-scan of M483Al base CMC/KAAP 57

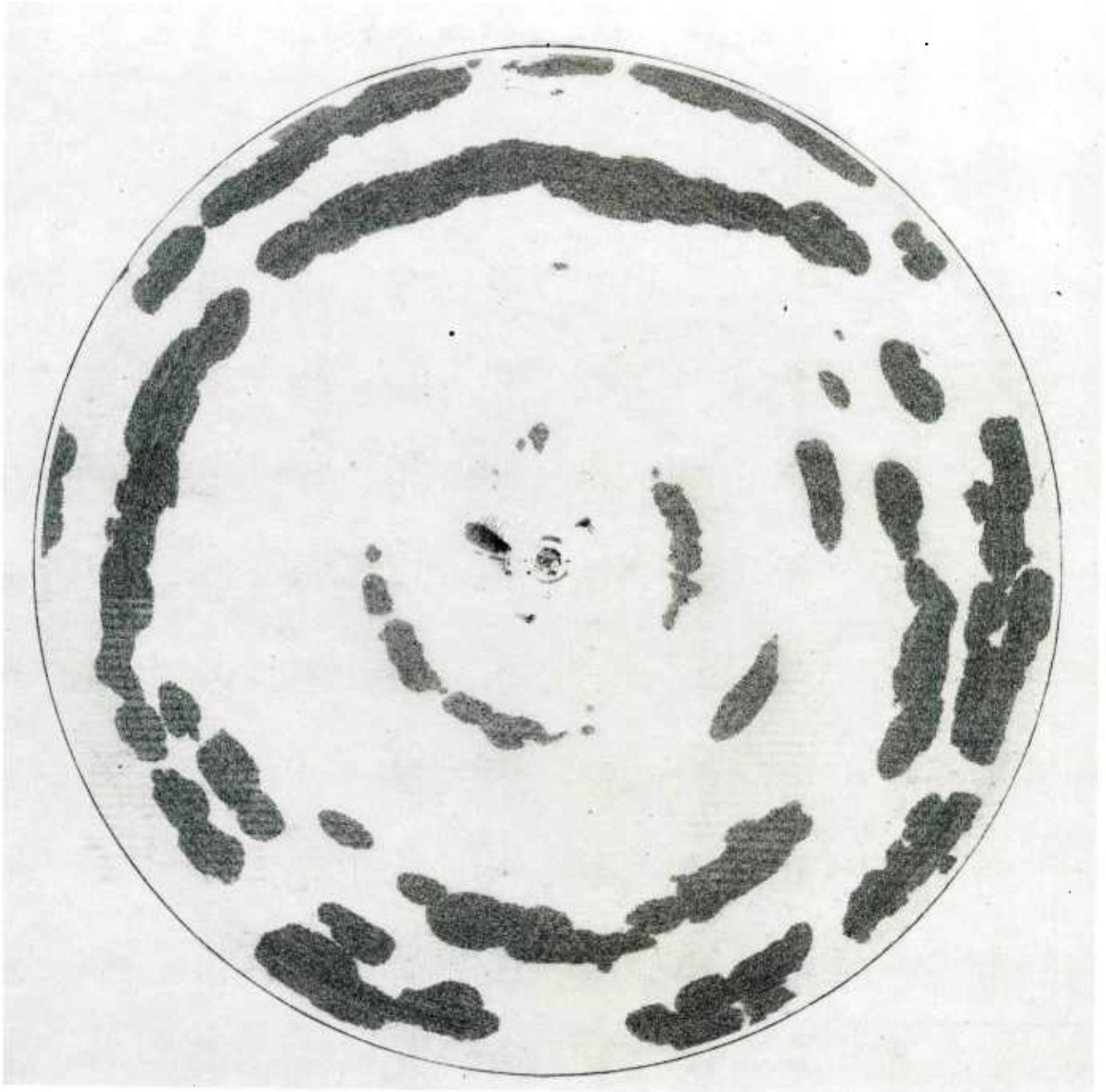


Figure 11. Ultrasonic C-scan of M483A1 base CMC/KAAP 61

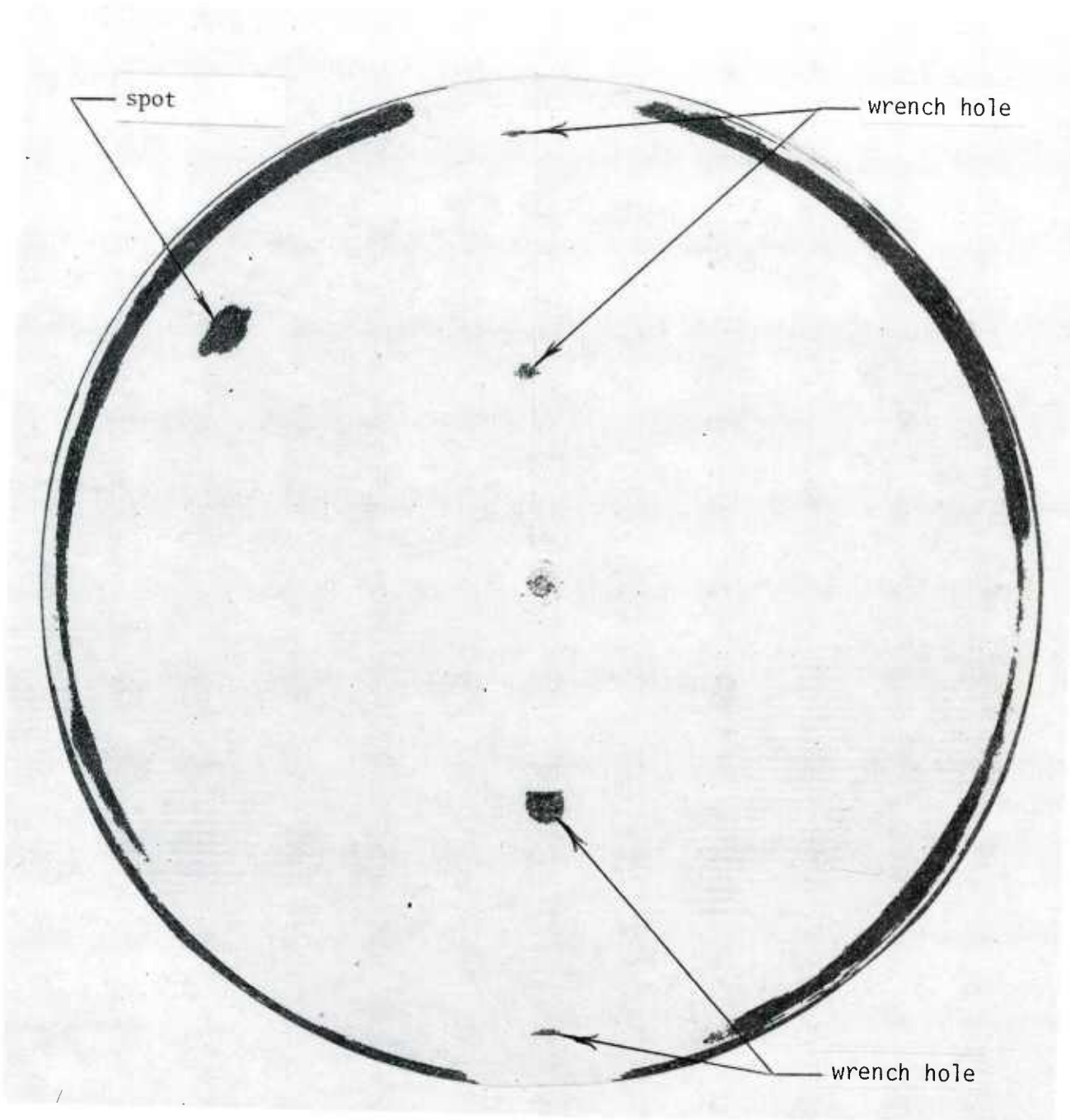


Figure 12. Ultrasonic C-scan of M483A1 base CMC/KAAP 62



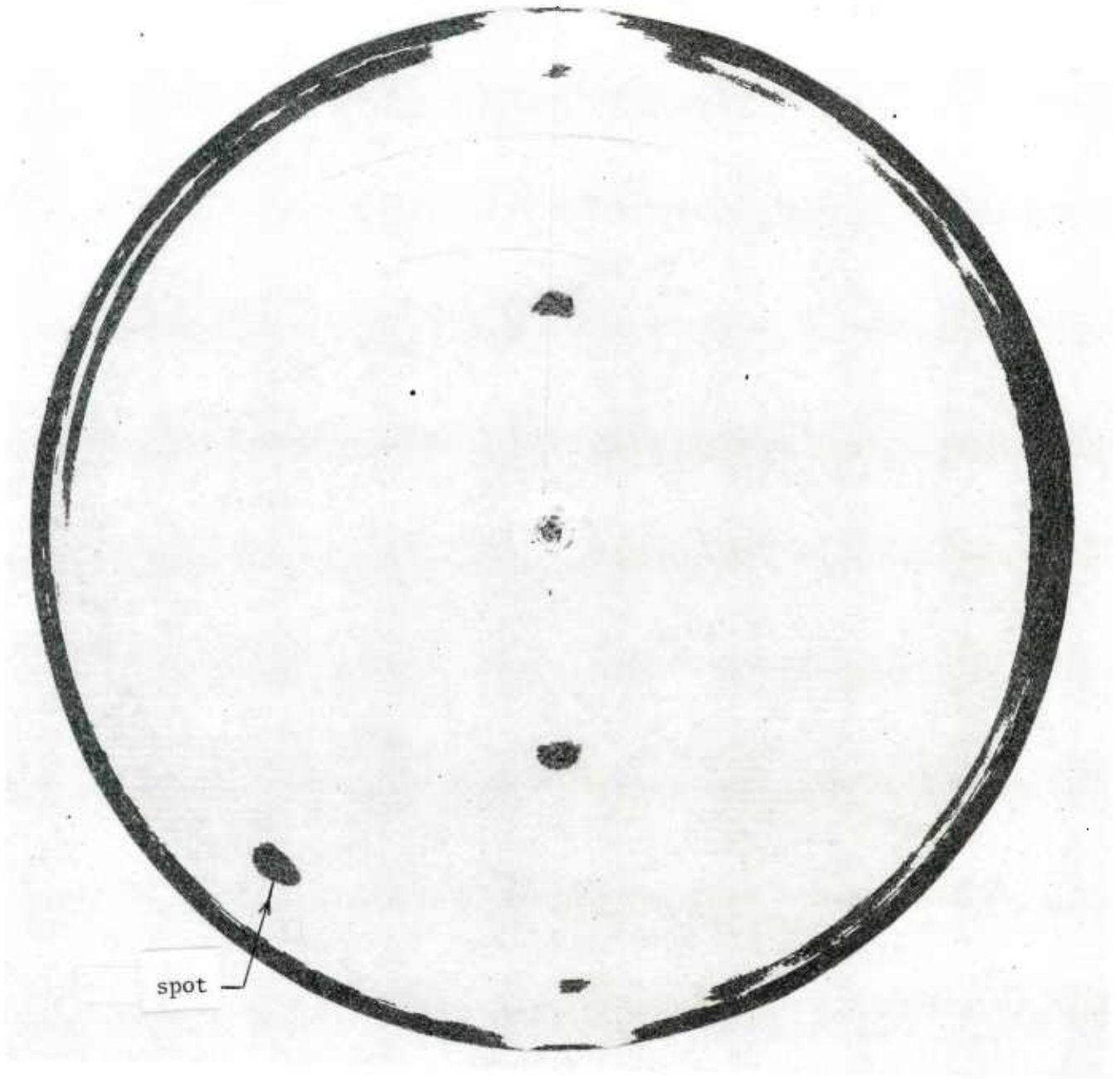


Figure 13. Ultrasonic C-scan of M483A1 base CMC/KAAP 63

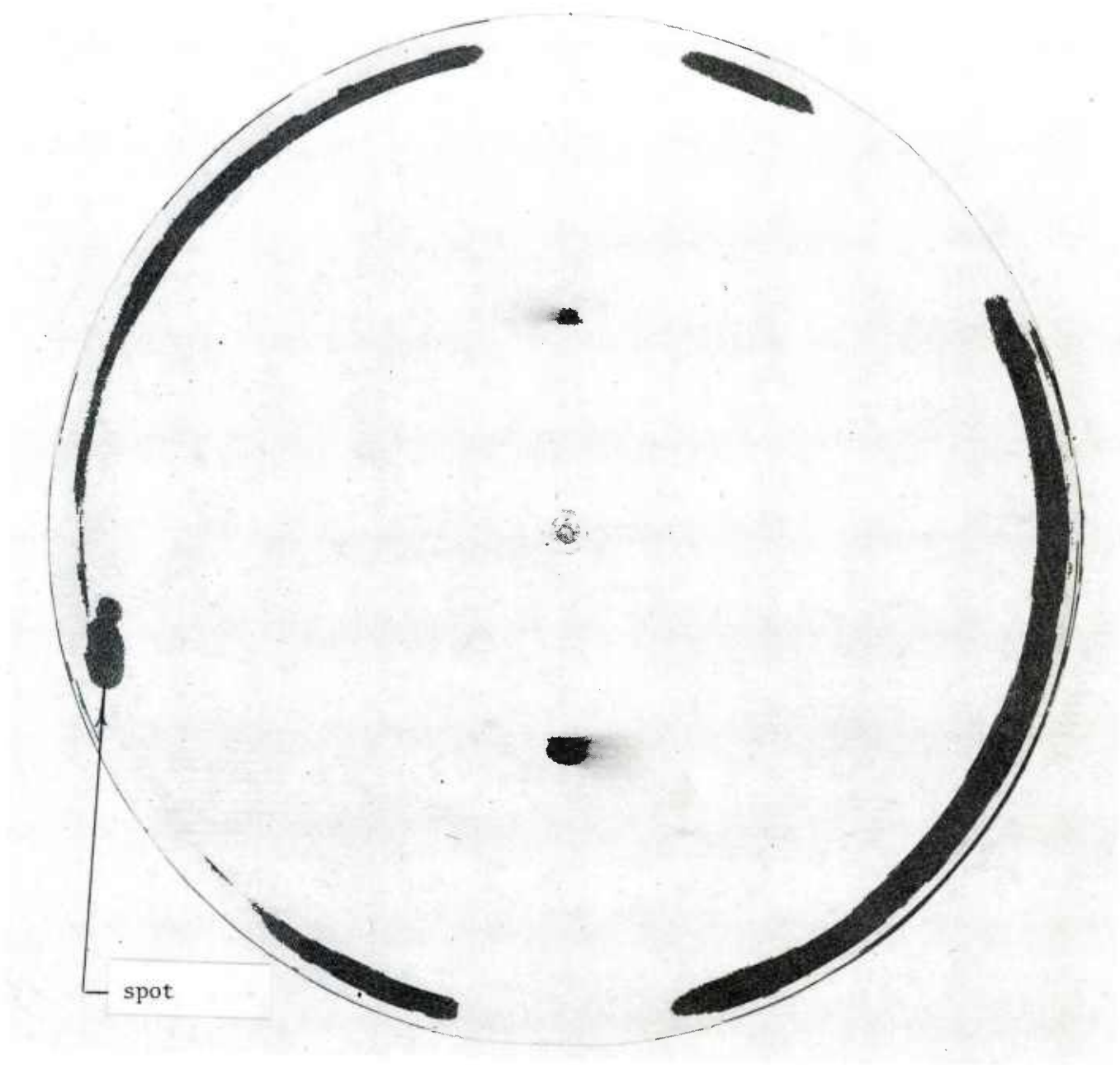


Figure 14. Ultrasonic C-scan of M483A1 base CMC/KAAP 64

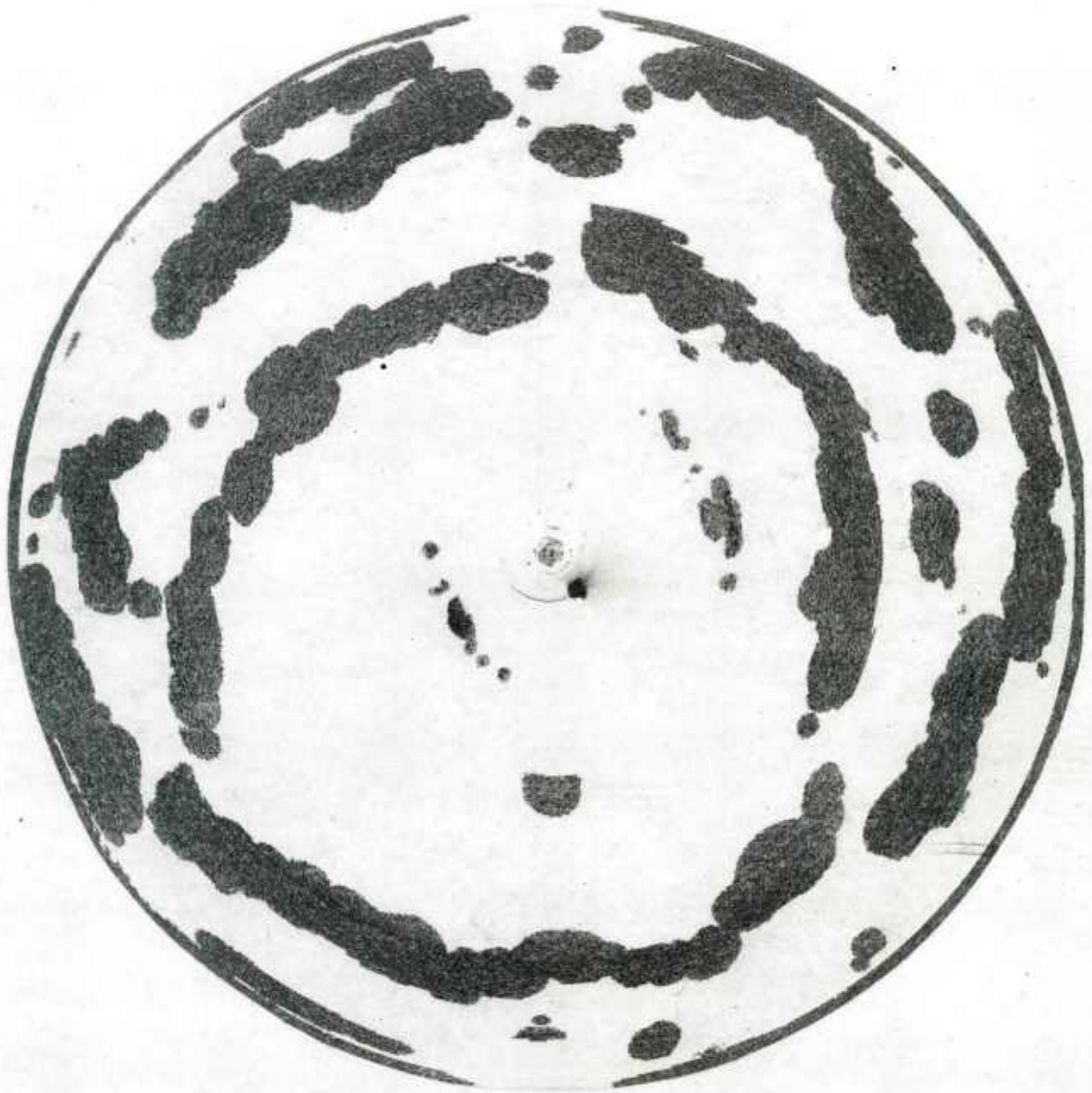


Figure 15. Ultrasonic C-scan of M483A1 base CMC/KAAP 65



Figure 16. Ultrasonic C-scan of M483A1 base CMC/KAAP 66

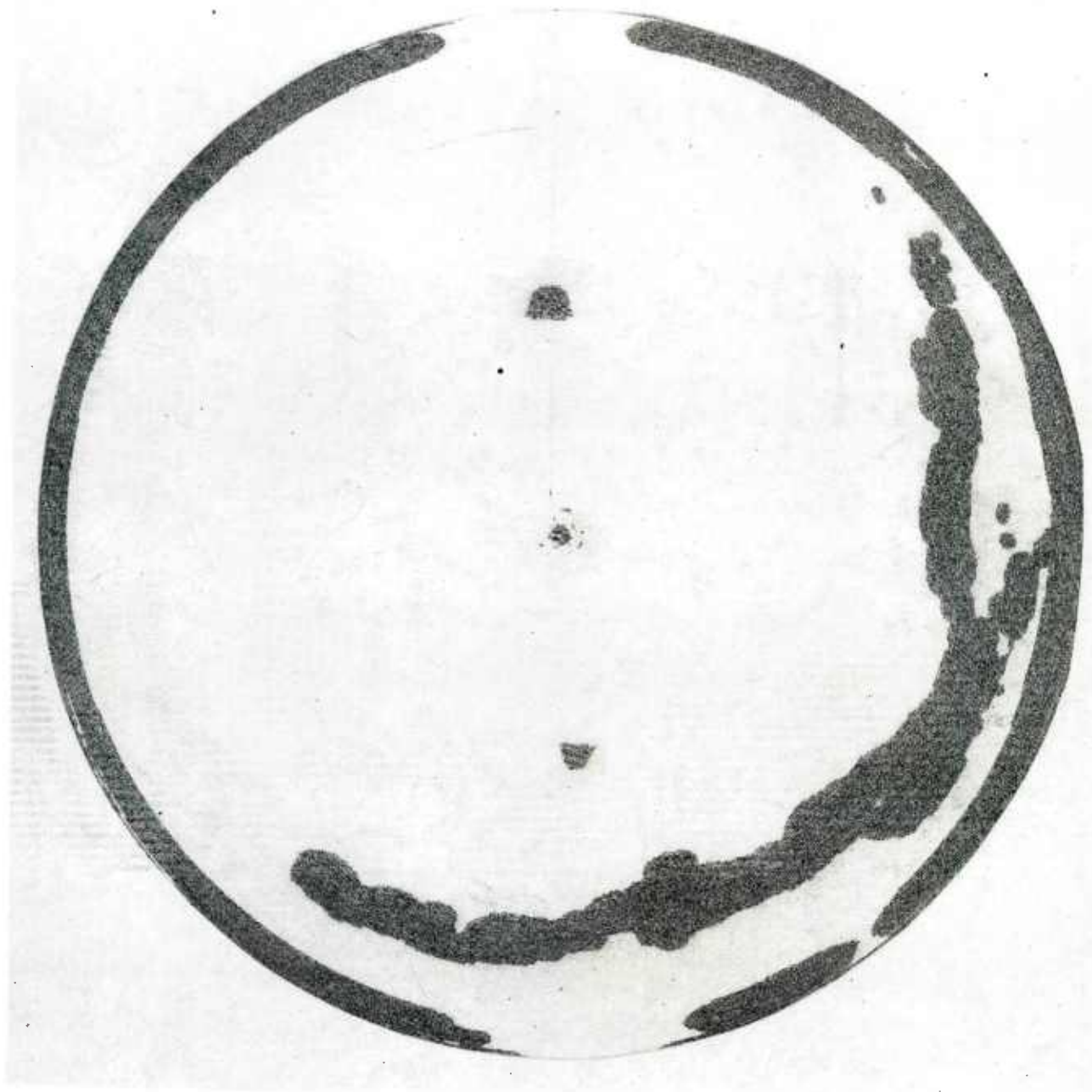


Figure 17. Ultrasonic C-scan of M483A1 base CMC/KAAP 68

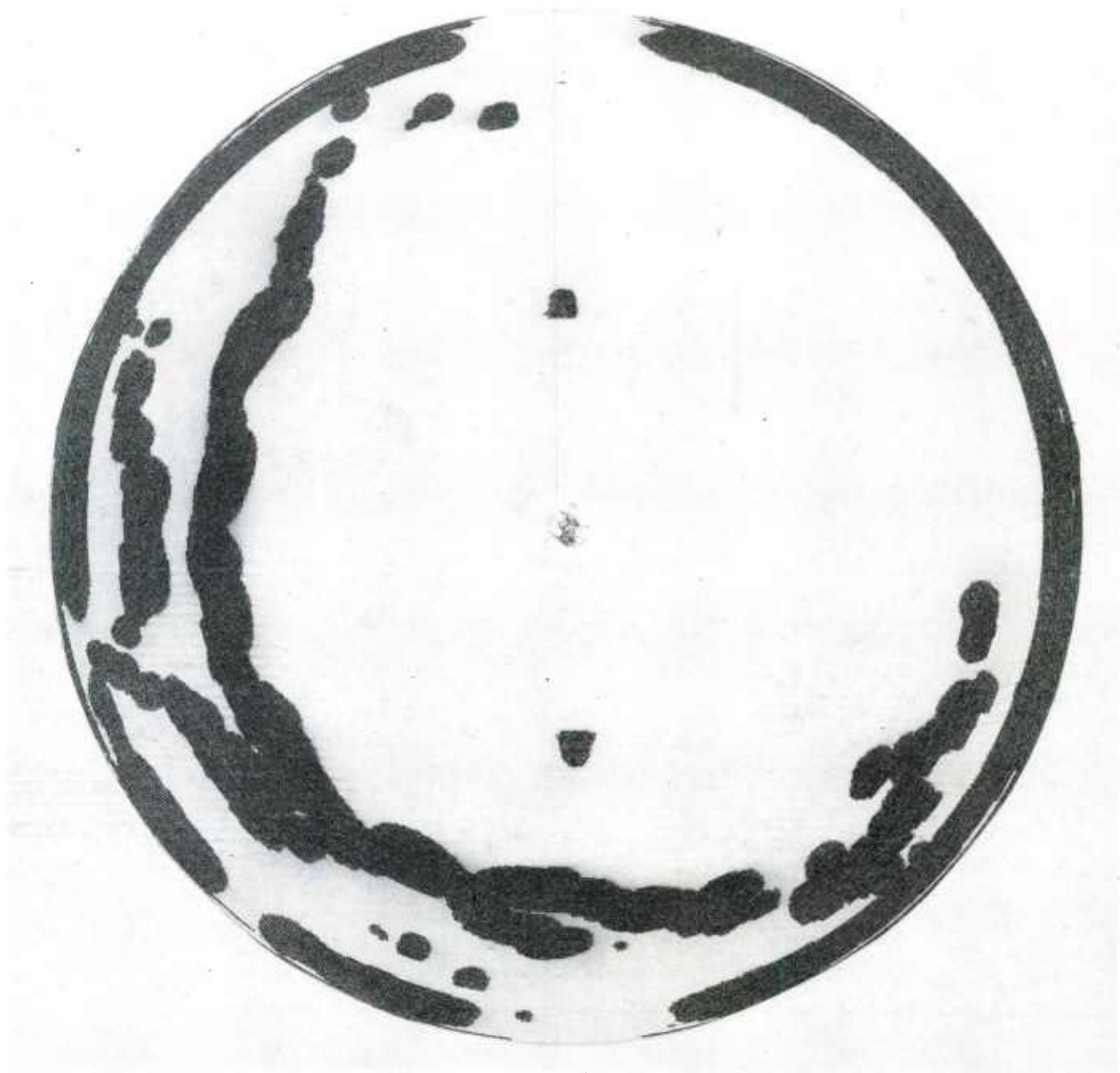


Figure 18. Ultrasonic C-scan of M483A1 base CMC/KAAP 70

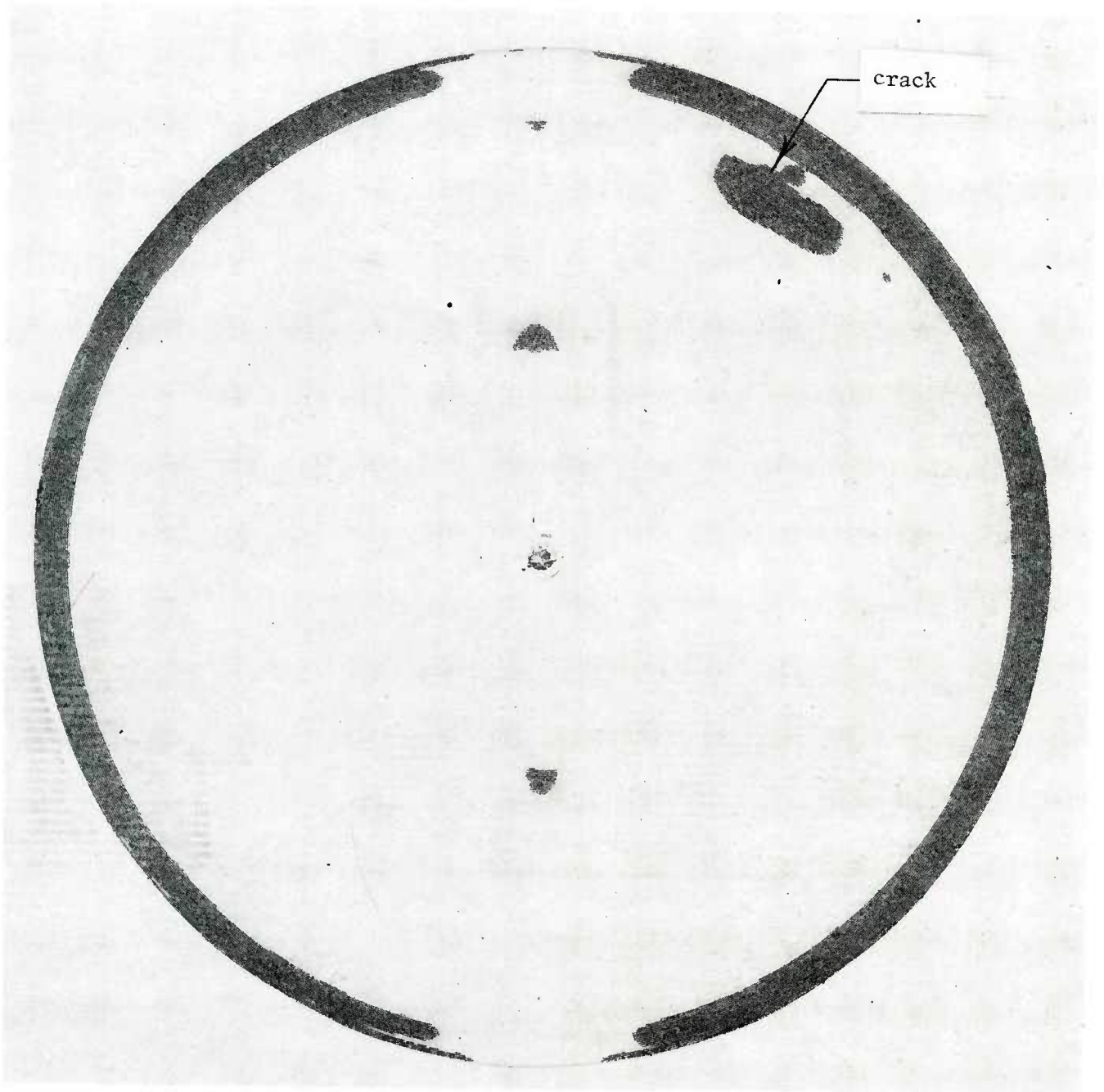


Figure 19. Ultrasonic C-scan of M483Al base CMC/KAAP 71

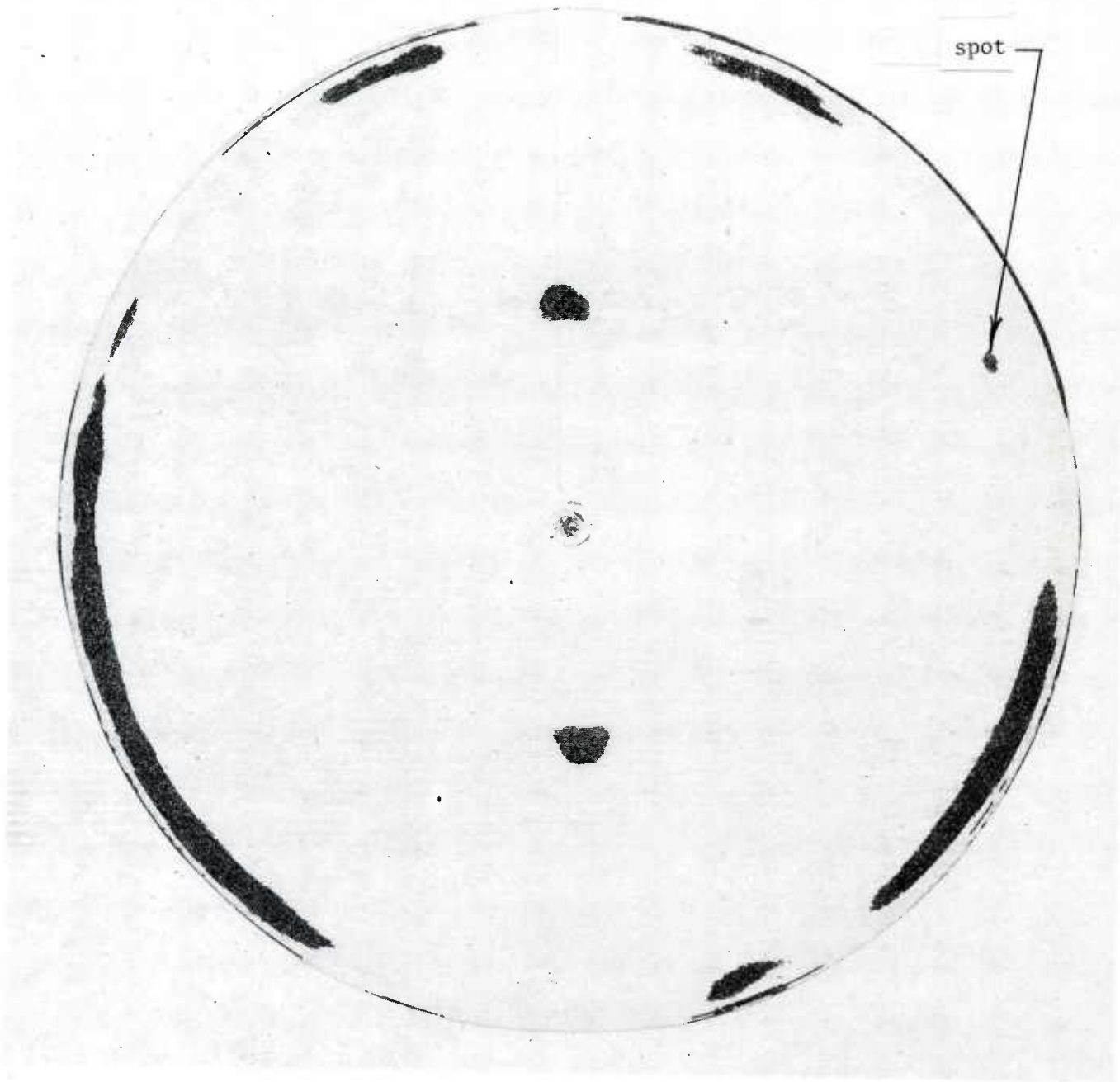


Figure 20. Ultrasonic C-scan of M483A1 base CMC/KAAP 75



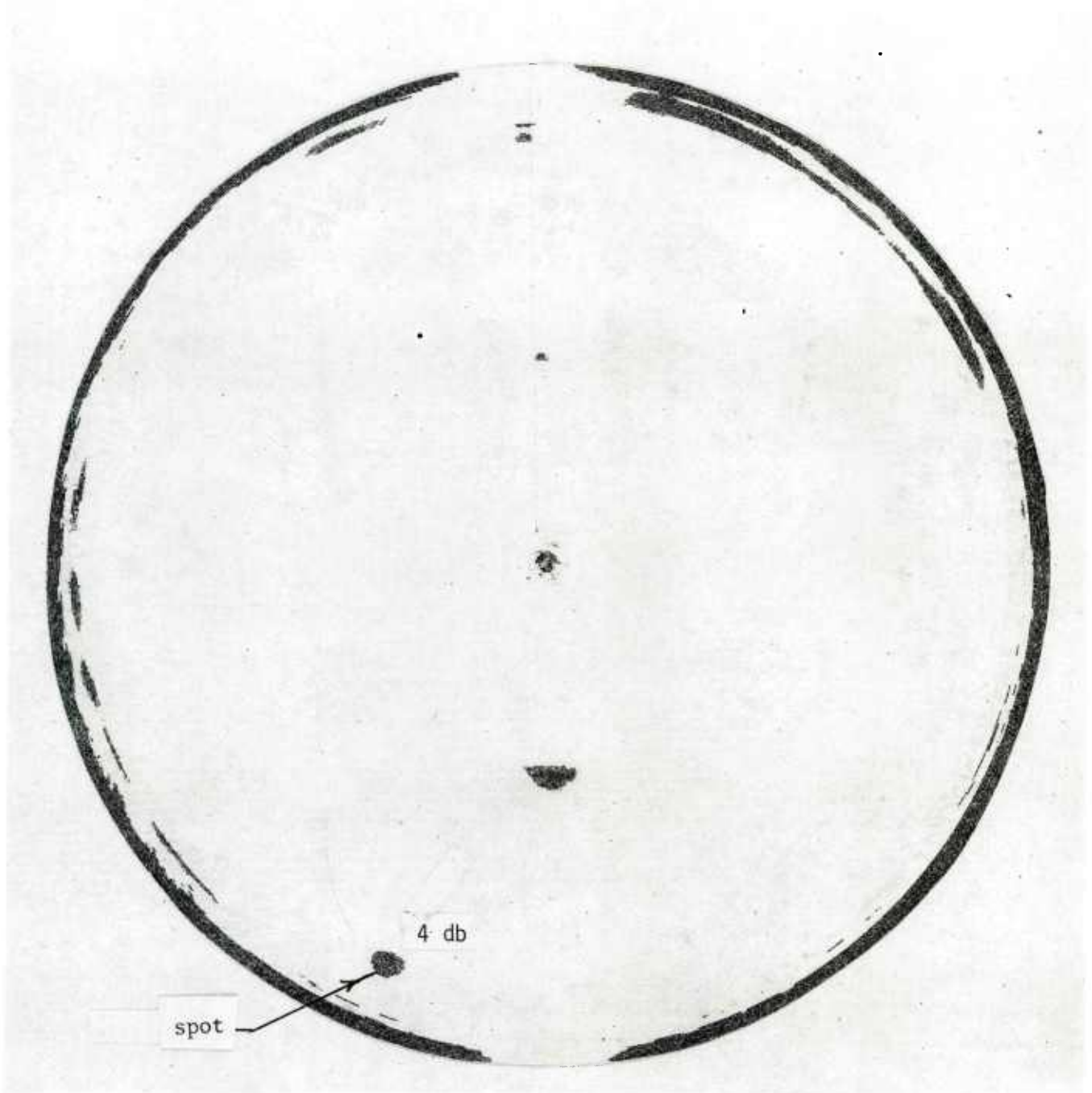


Figure 21. Ultrasonic C-scan of M483A1 base CMC/KAAP 76

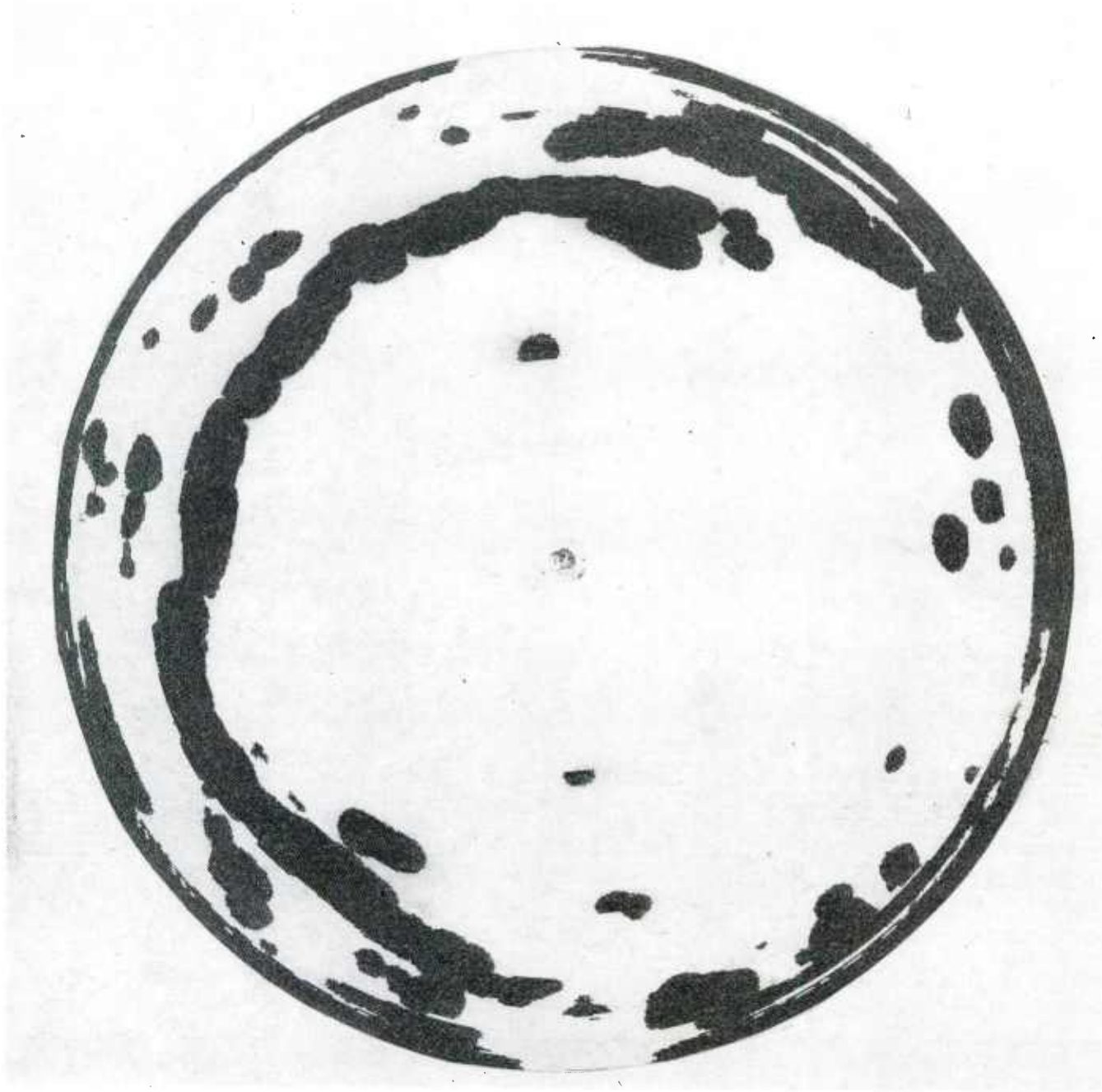


Figure 22. Ultrasonic C-scan of M483A1 base CMC/KAAP 125

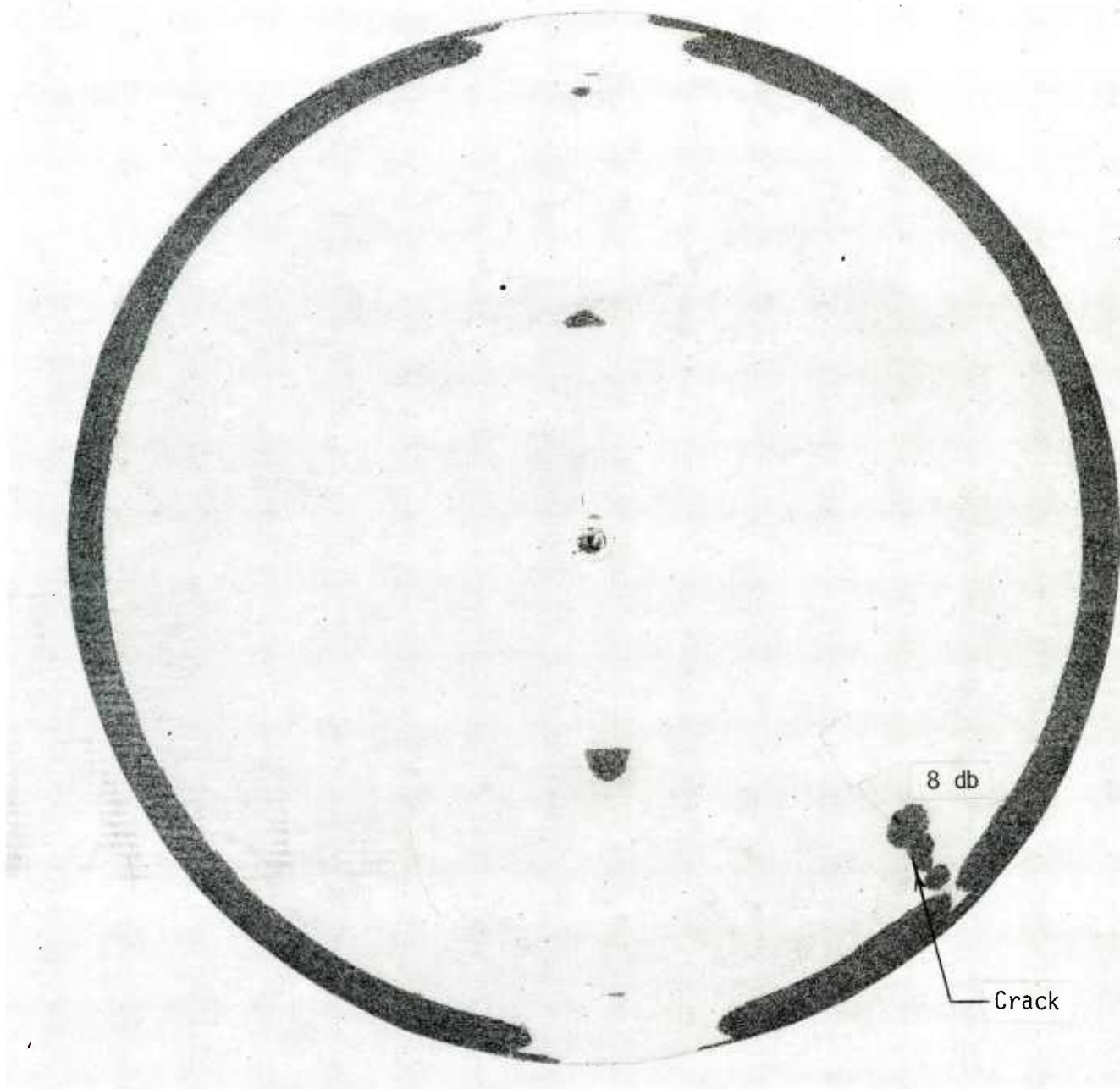


Figure 23. Ultrasonic C-scan of M483Al base CMC/LSAAP 296

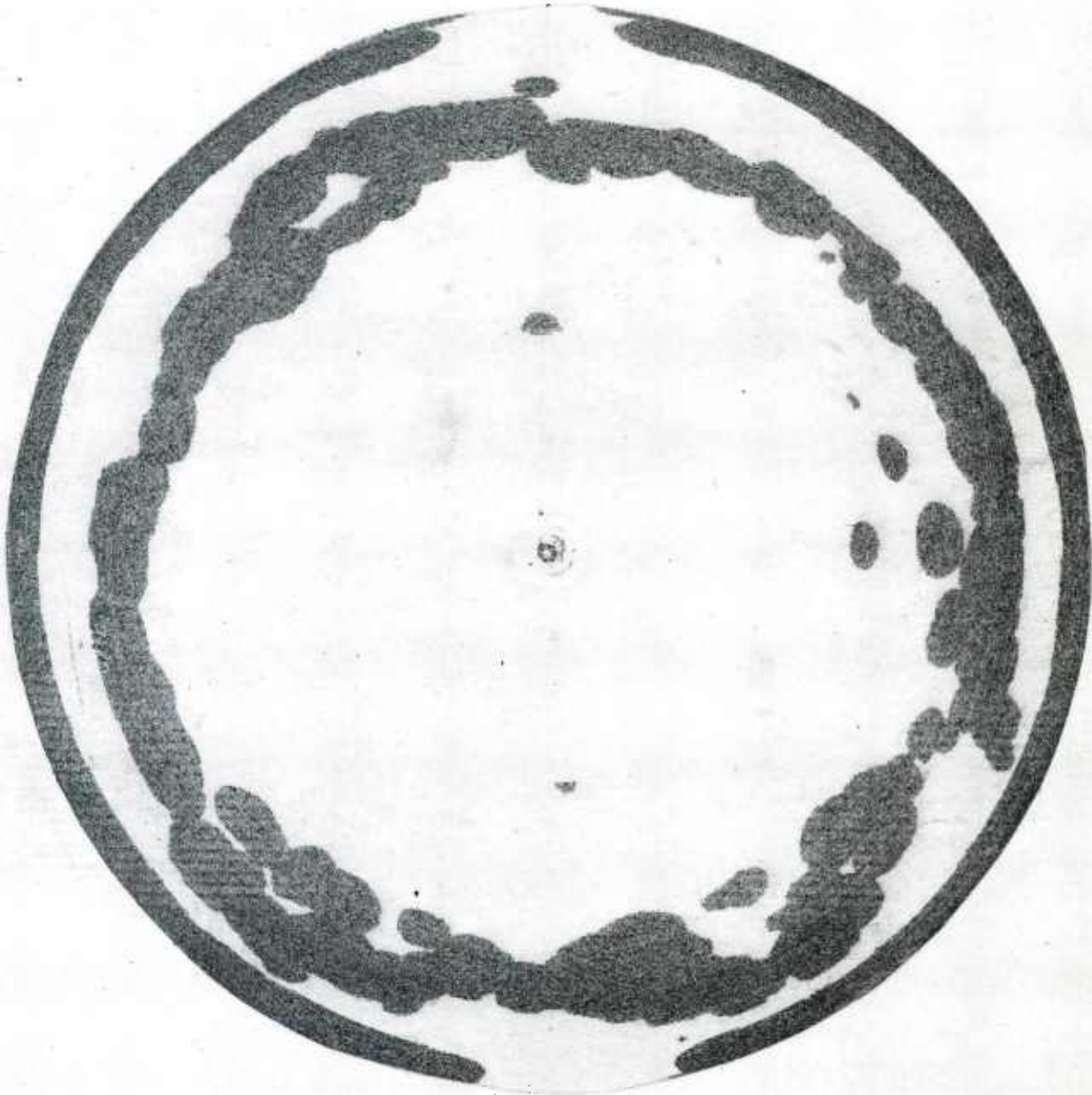


Figure 24. Ultrasonic C-scan of M483A1 base CMC/LSAAP 303

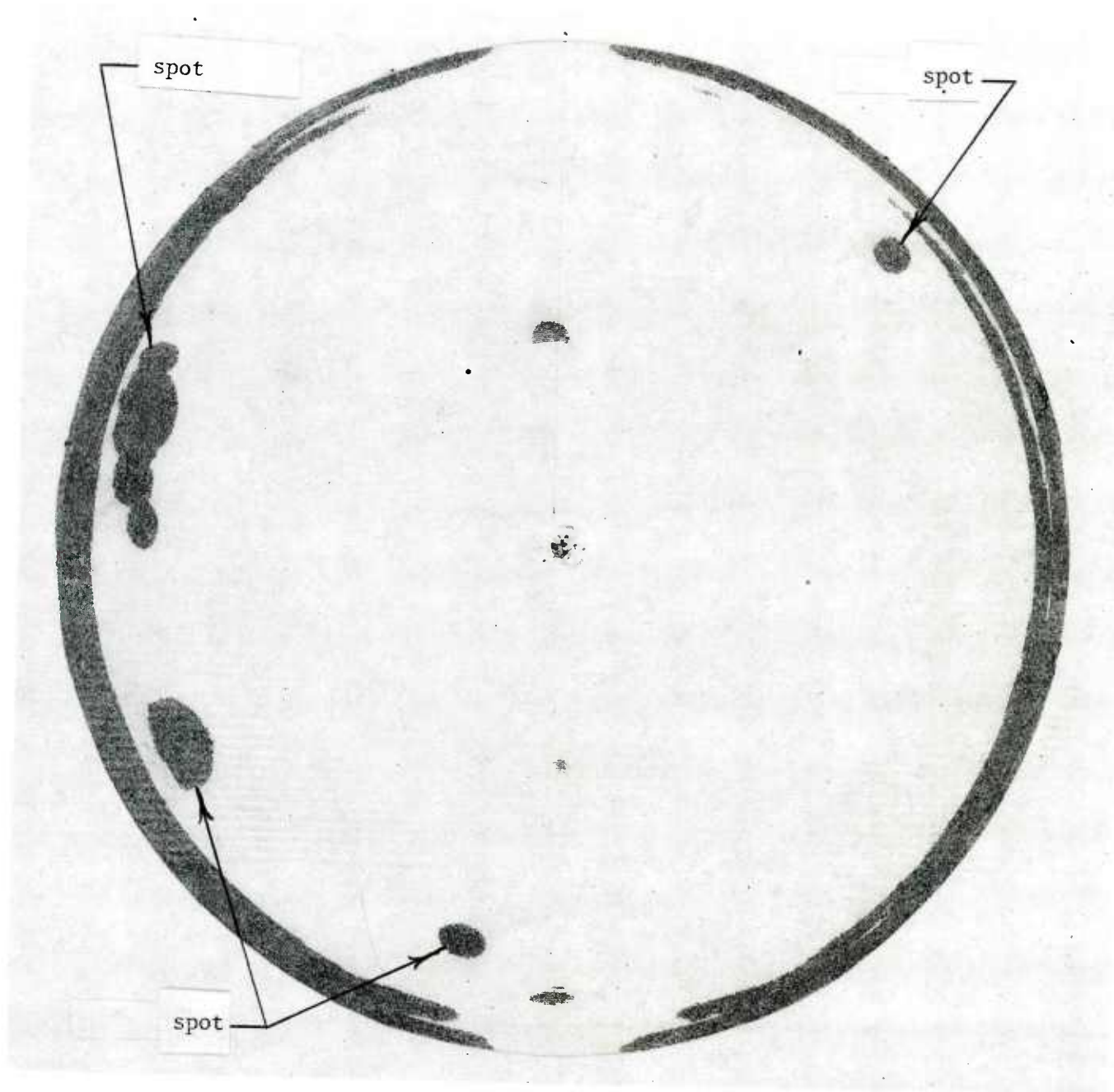


Figure 25. Ultrasonic C-scan of M483A1 base CMC/LSAAP 305

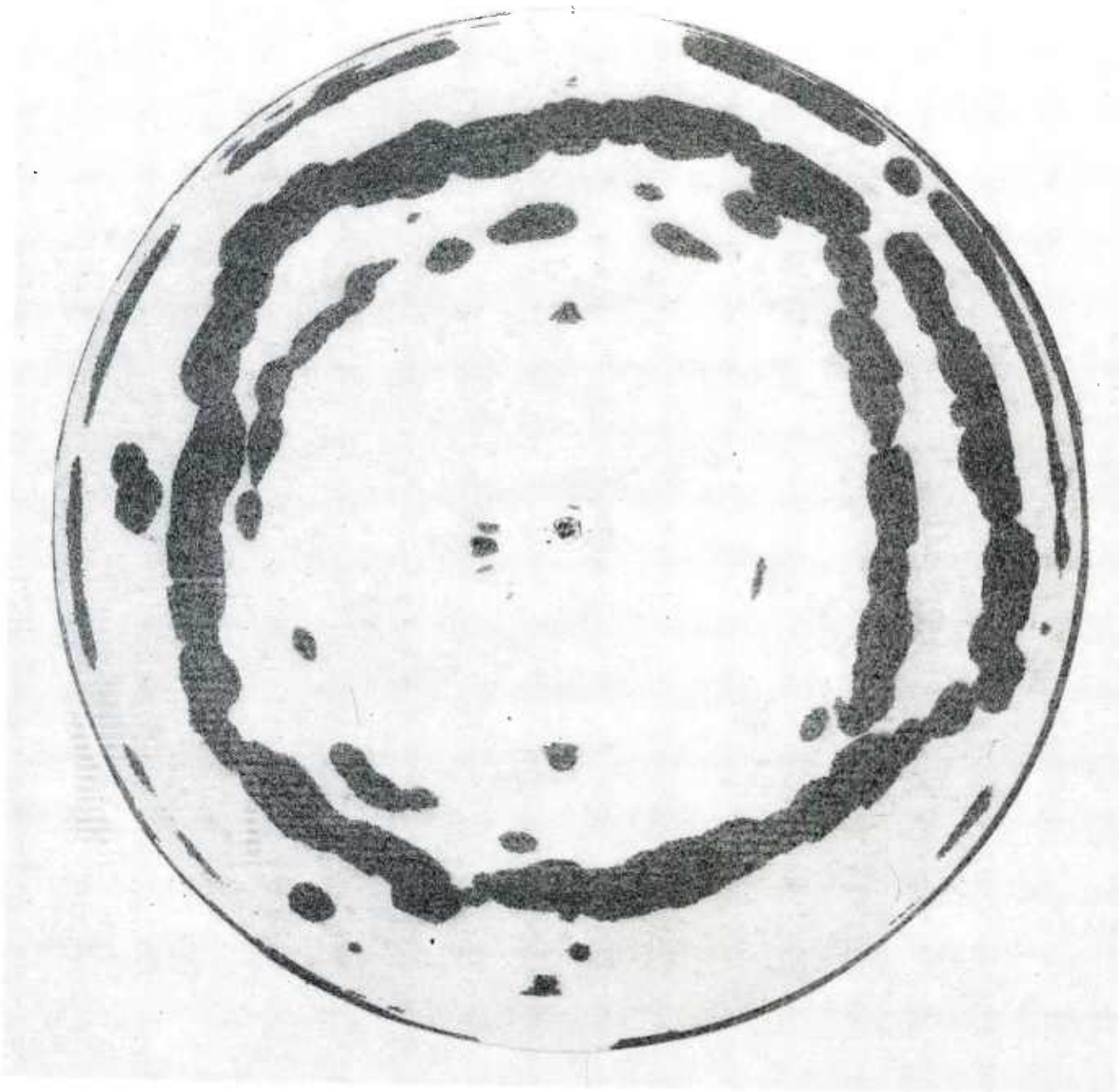


Figure 26. Ultrasonic C-scan of M483A1 base CMC/LSAAP 306

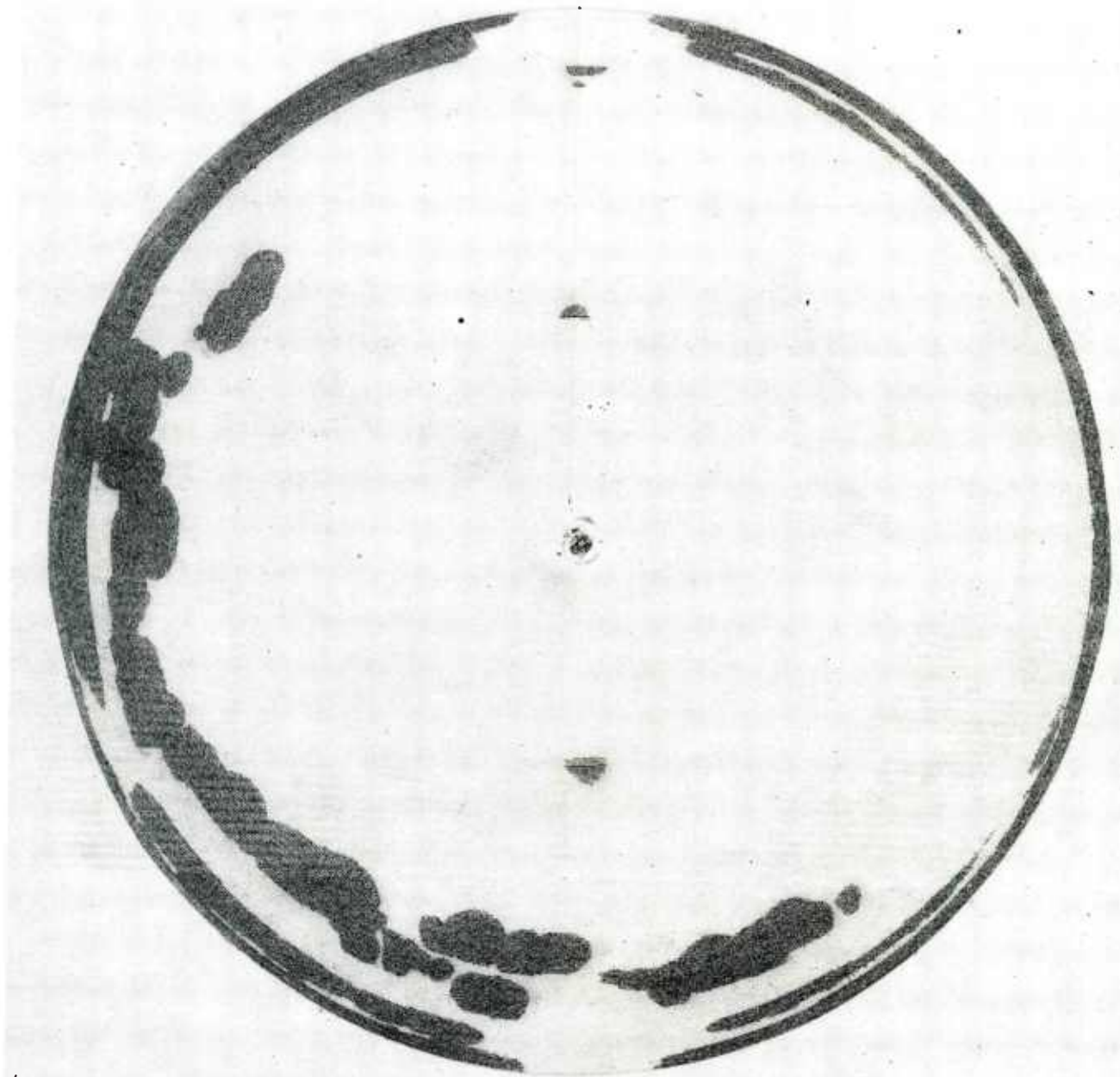


Figure 27. Ultrasonic C-scan of M483A1 base CMC/LSAAP 307

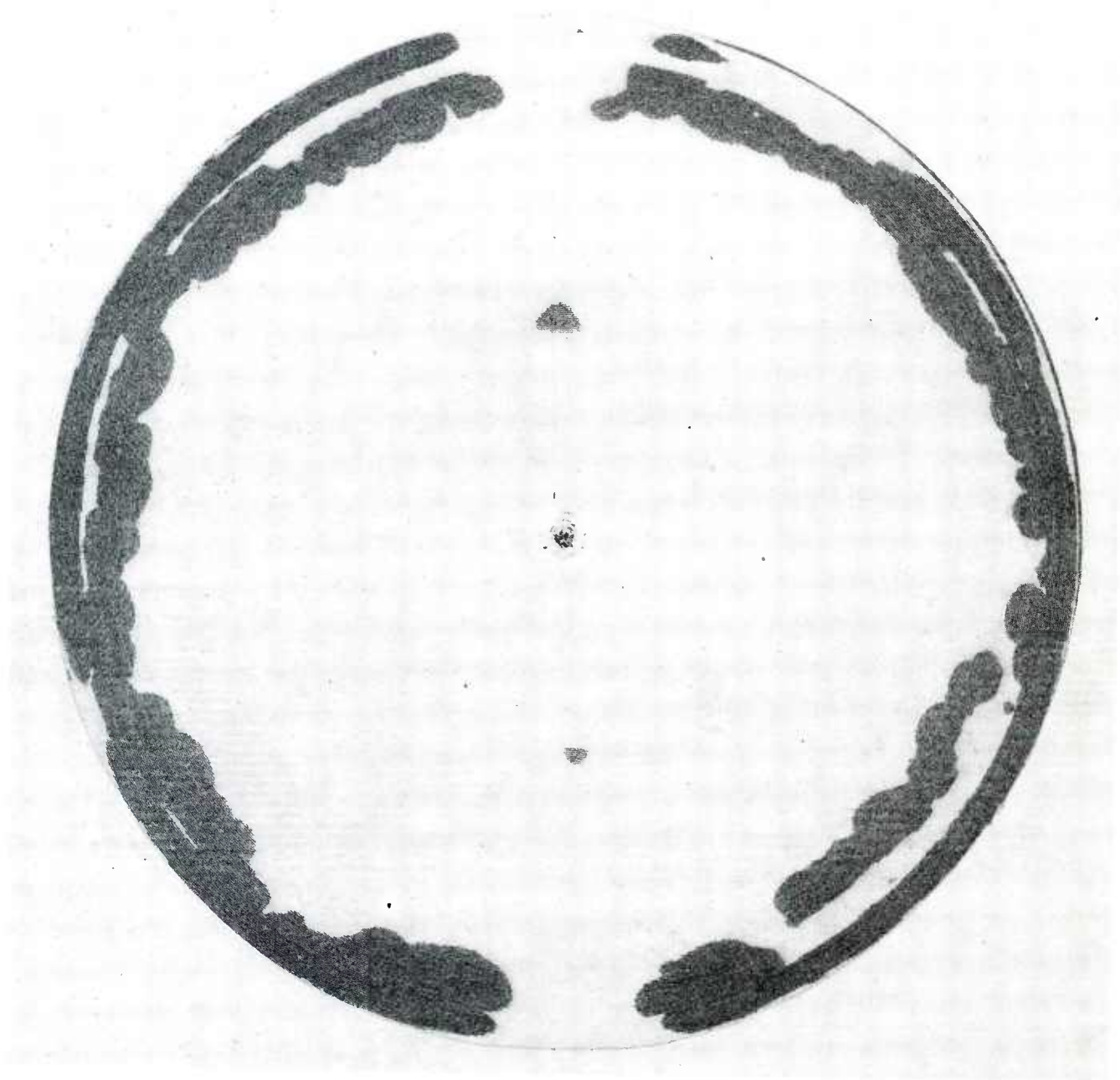


Figure 28. Ultrasonic C-scan of M483A1 base CMC/LSAAP 308



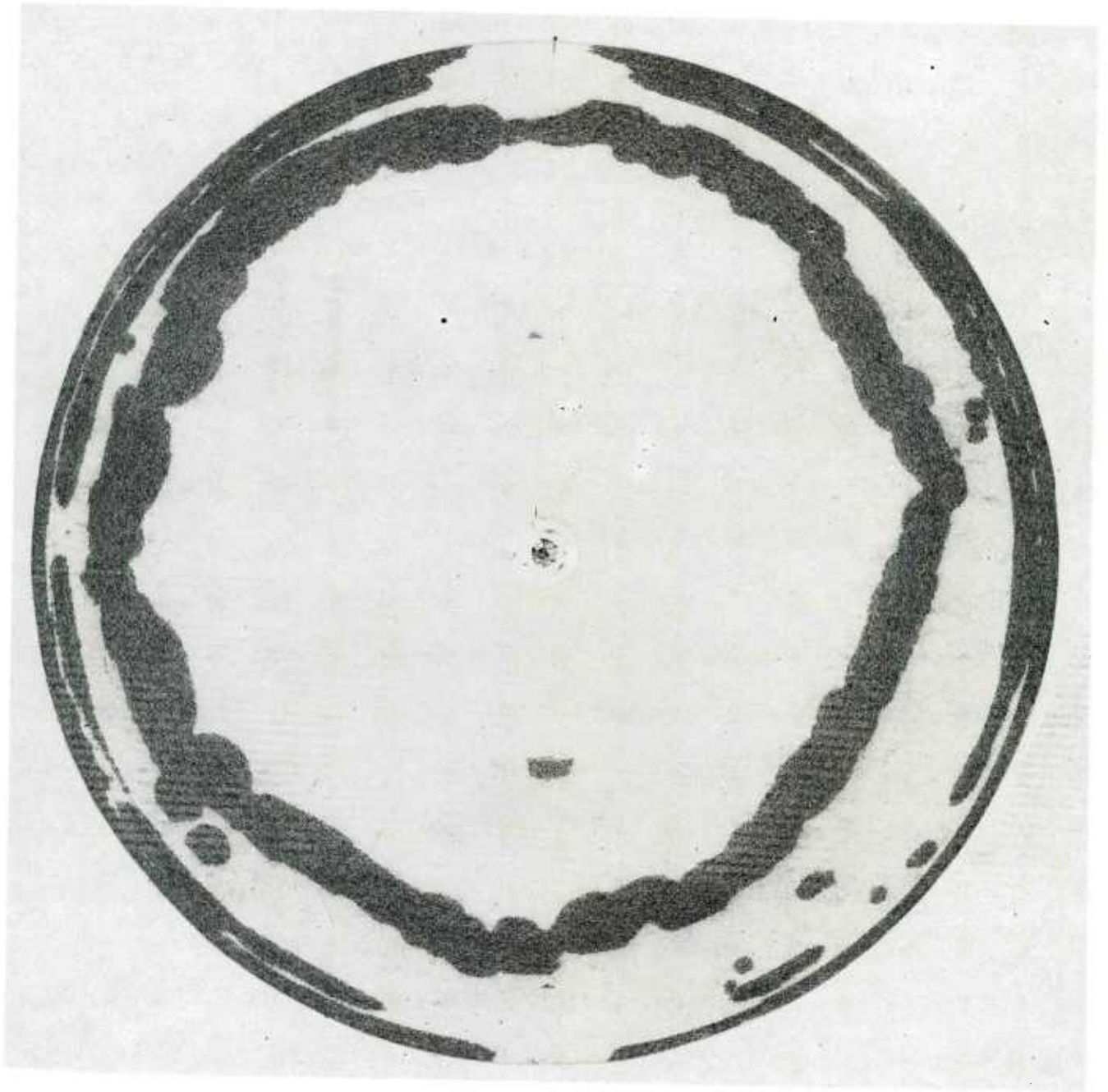


Figure 29. Ultrasonic C-scan of M483A1 base CMC/LSAAP 309

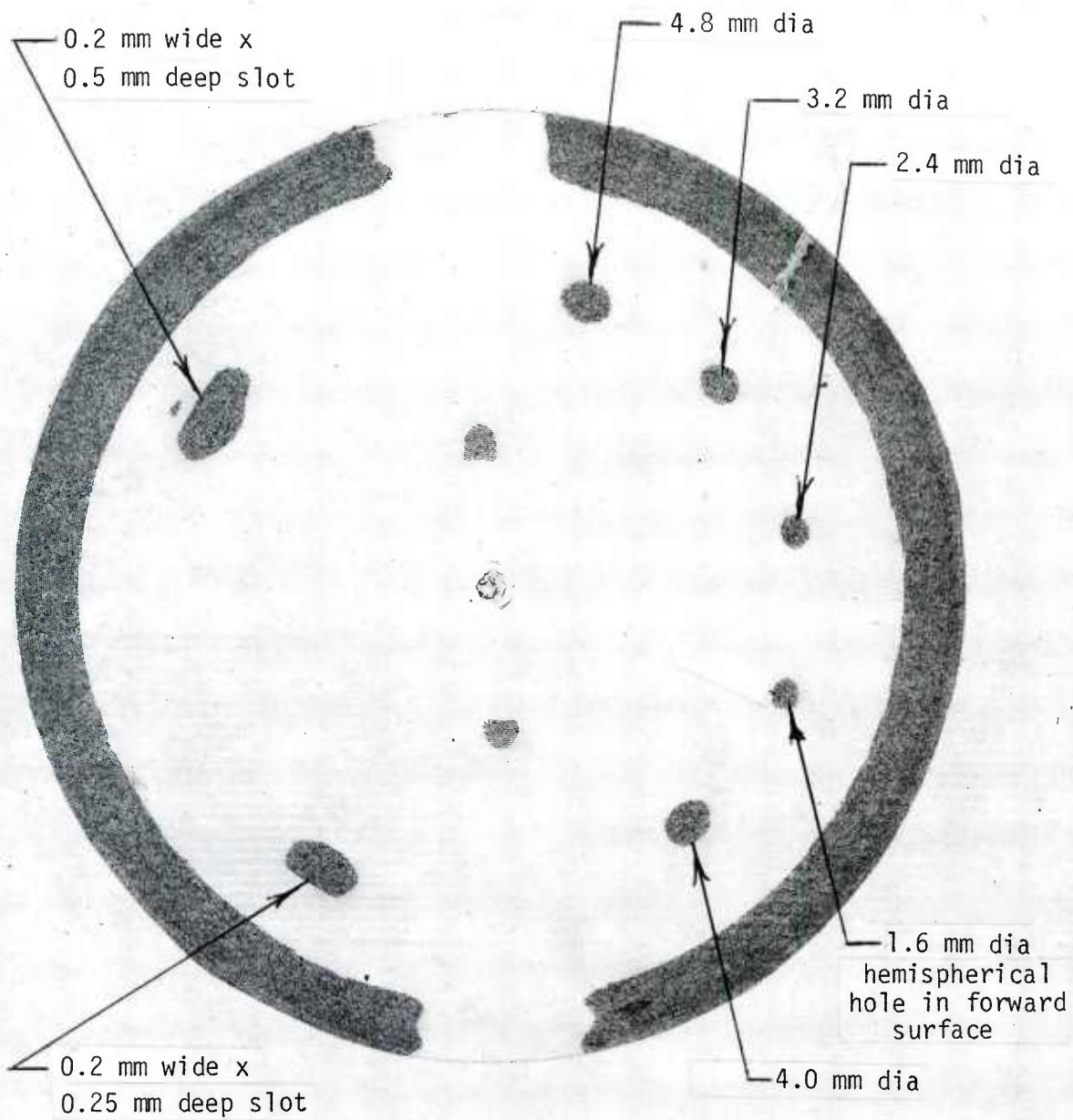


Figure 30. Ultrasonic C-scan of M483 base (standard)

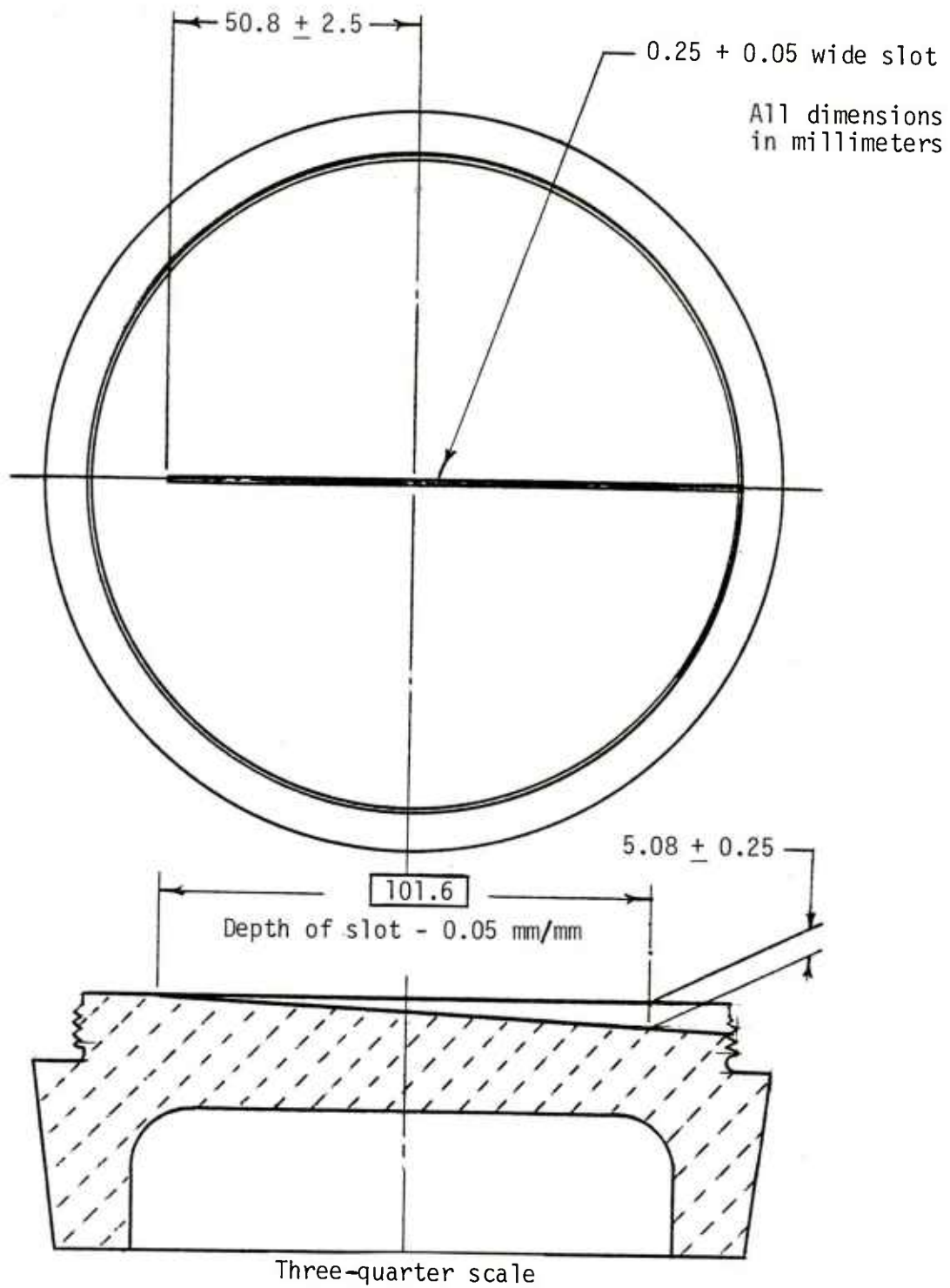


Figure 31. Eddy current standard with a variable-depth (inclined) slot in an M483A1 base

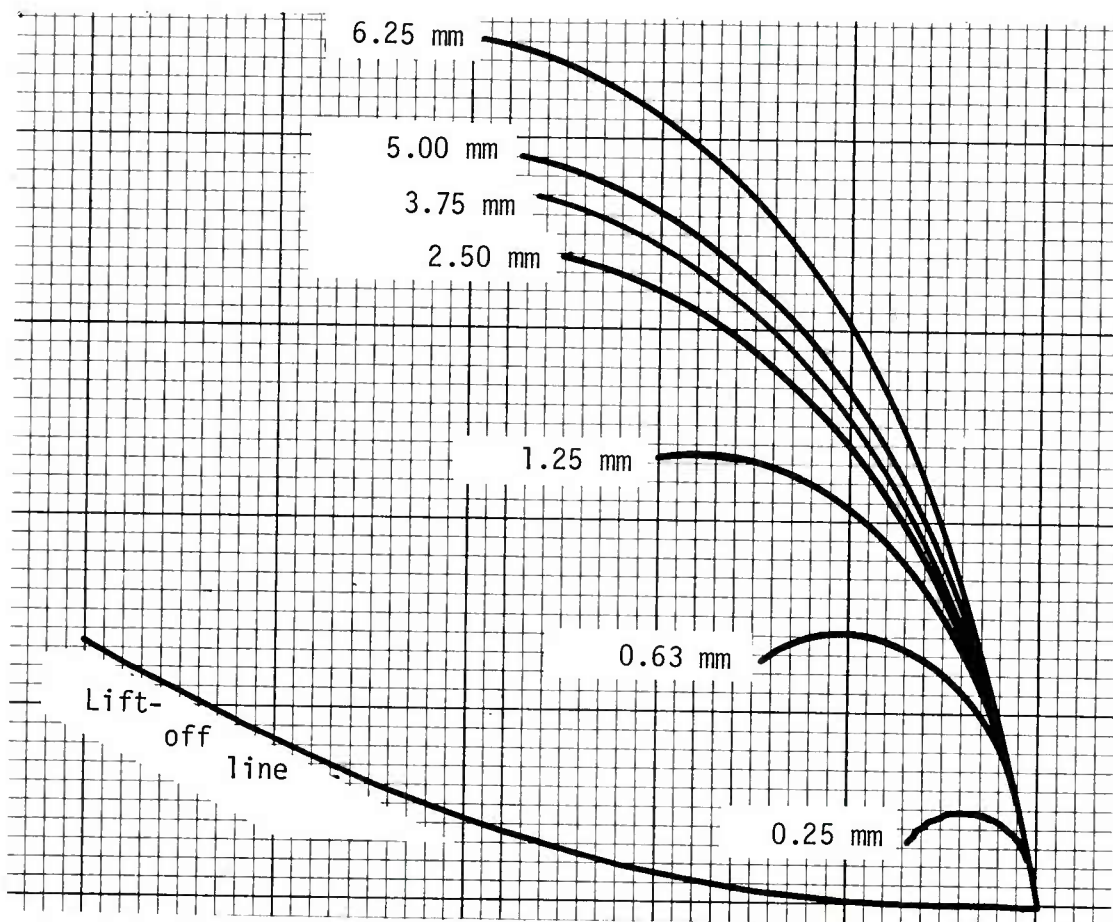
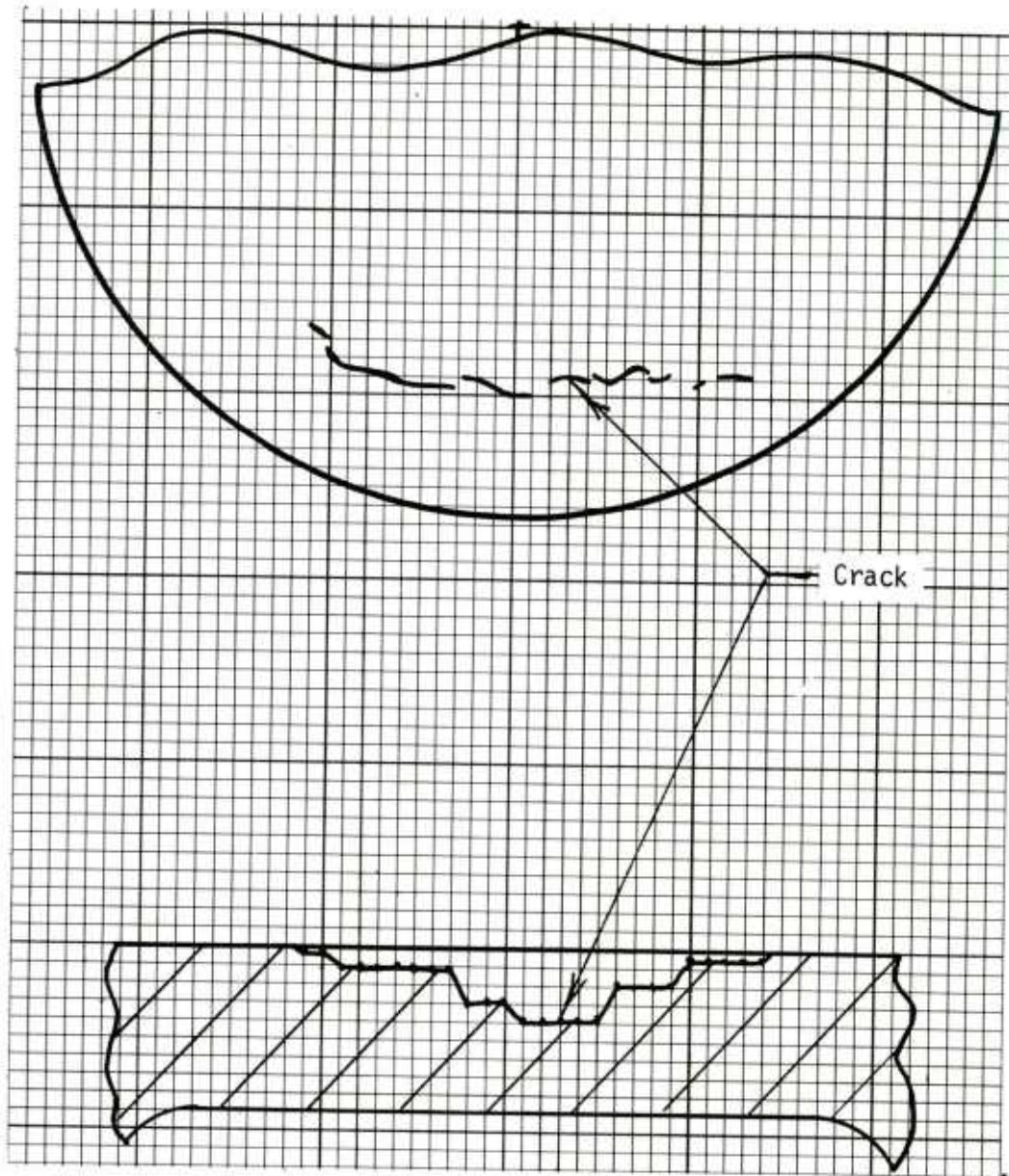


Figure 32. Vector dot trace for various depths of slots in the eddy current standard



Depth of crack  
drawn to double scale

Figure 33. Profile of crack in M692/M731 base A-CMC/LAAP 3

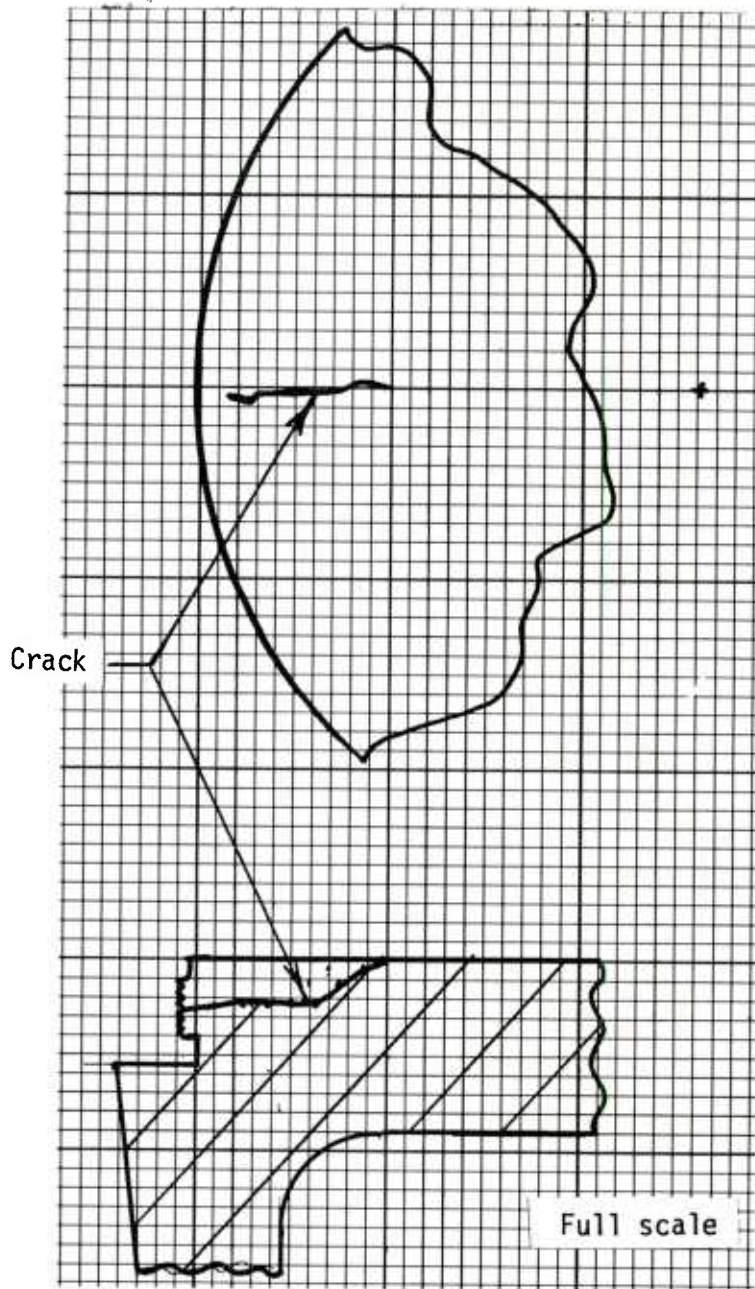
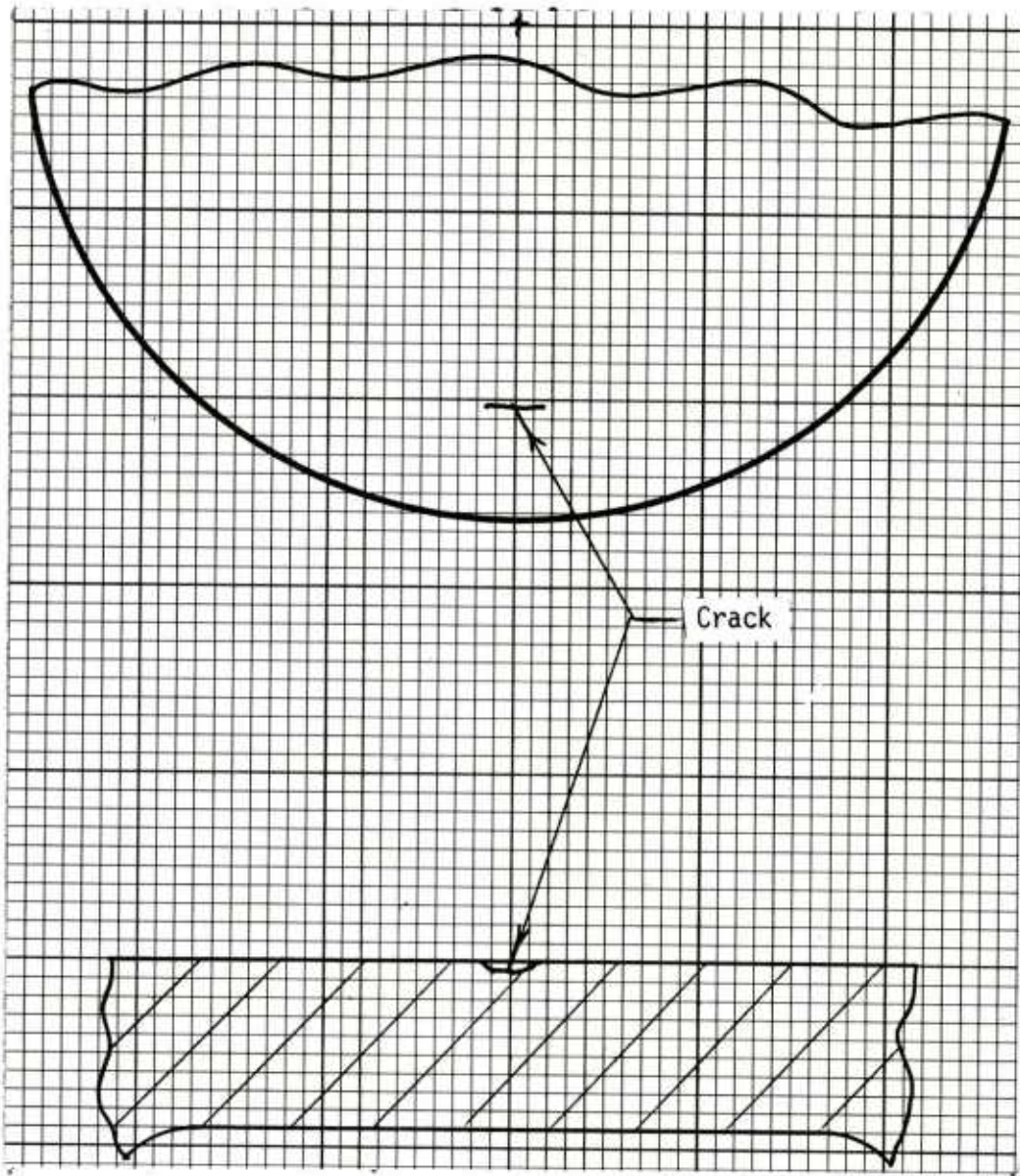
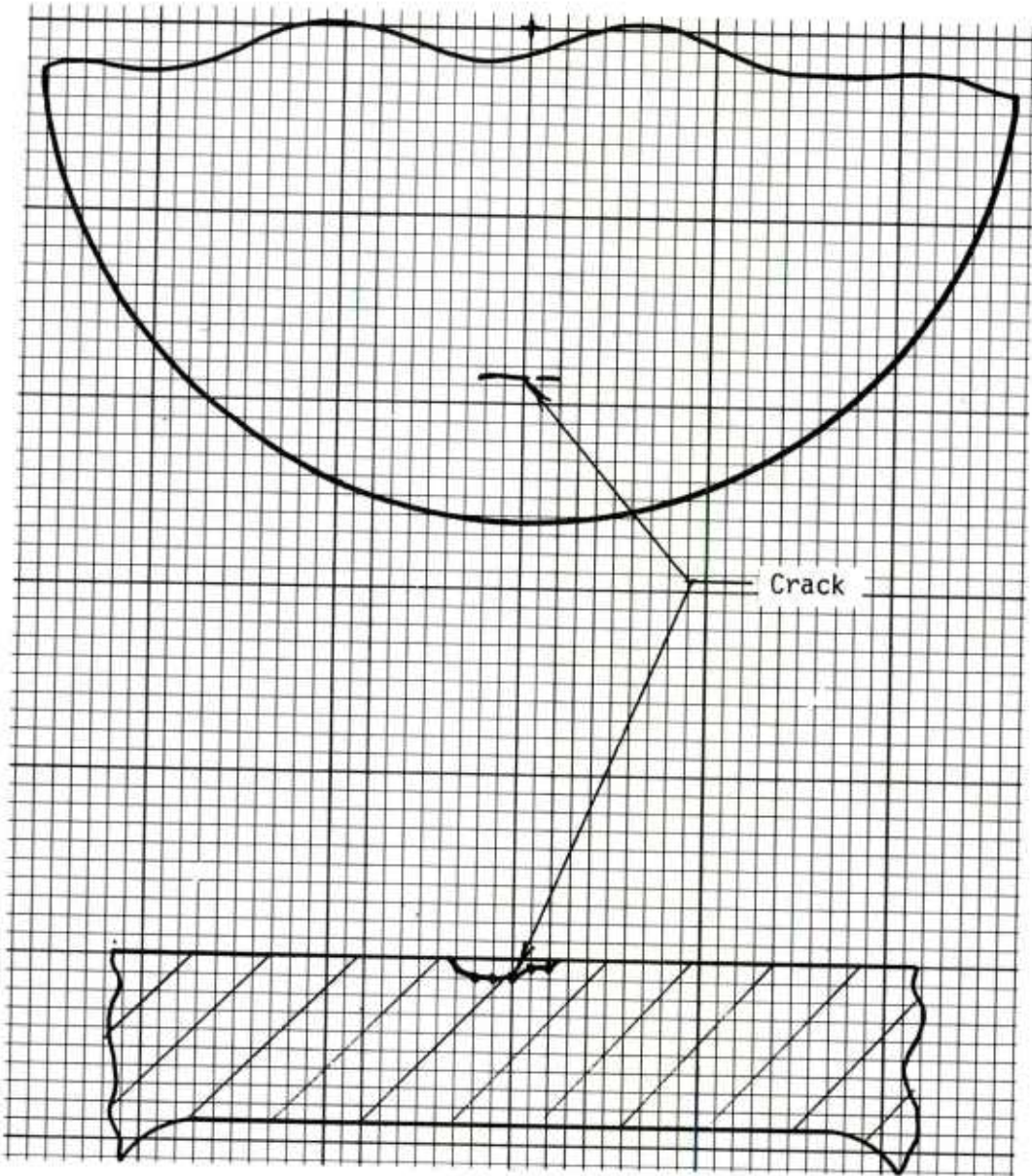


Figure 34. Profile of crack in M483Al base CMC/LSAAP 296



Depth of crack  
drawn to double scale

Figure 35. Profile of crack in M692/M731 base A-CMC/LAAP 4



Depth of crack  
drawn to double scale

Figure 36. Profile of crack in M483A1 base CMC/KAAP 71



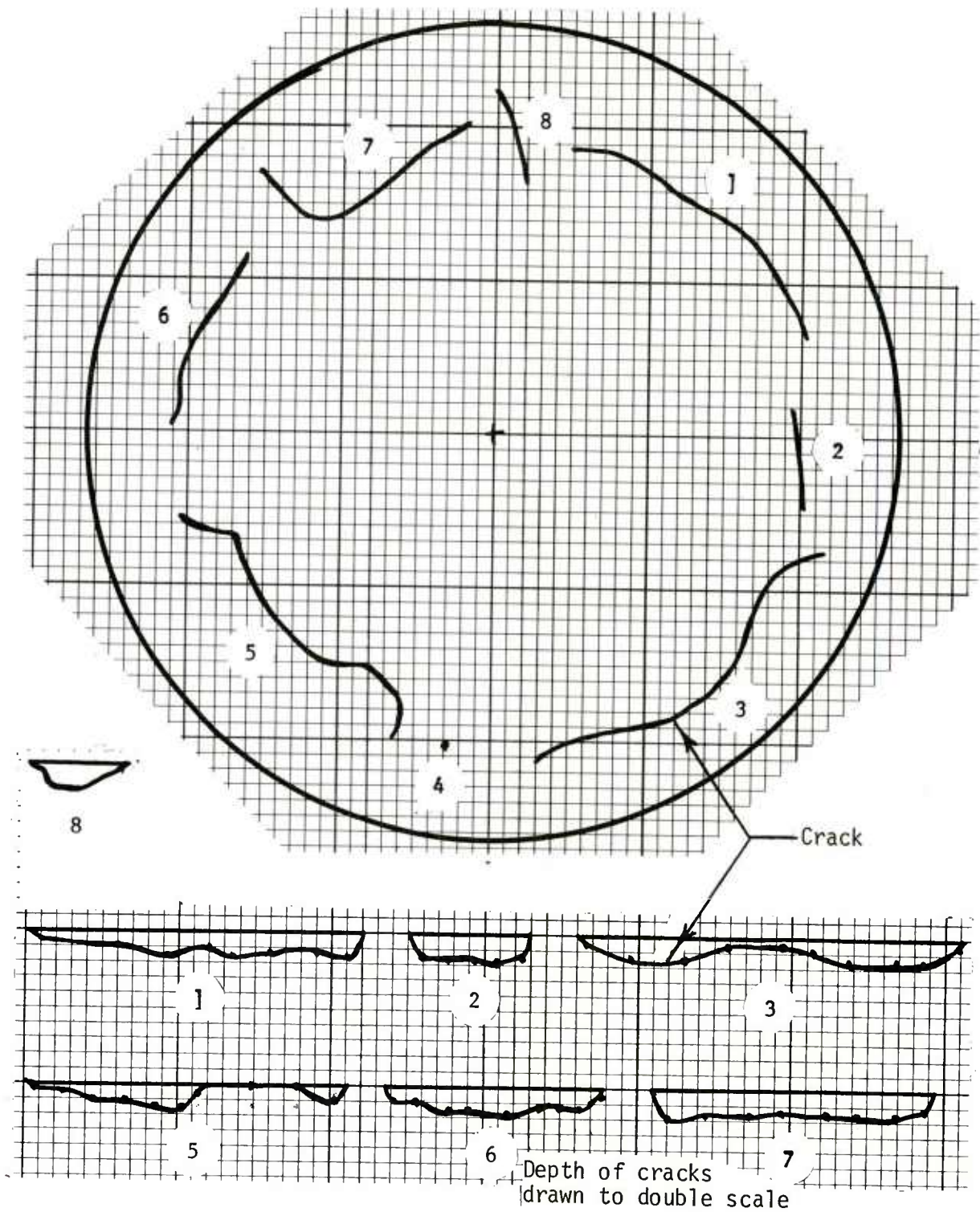


Figure 37. Profiles of cracks viewed from outside of M483A1 base CMC/LSAAP 308

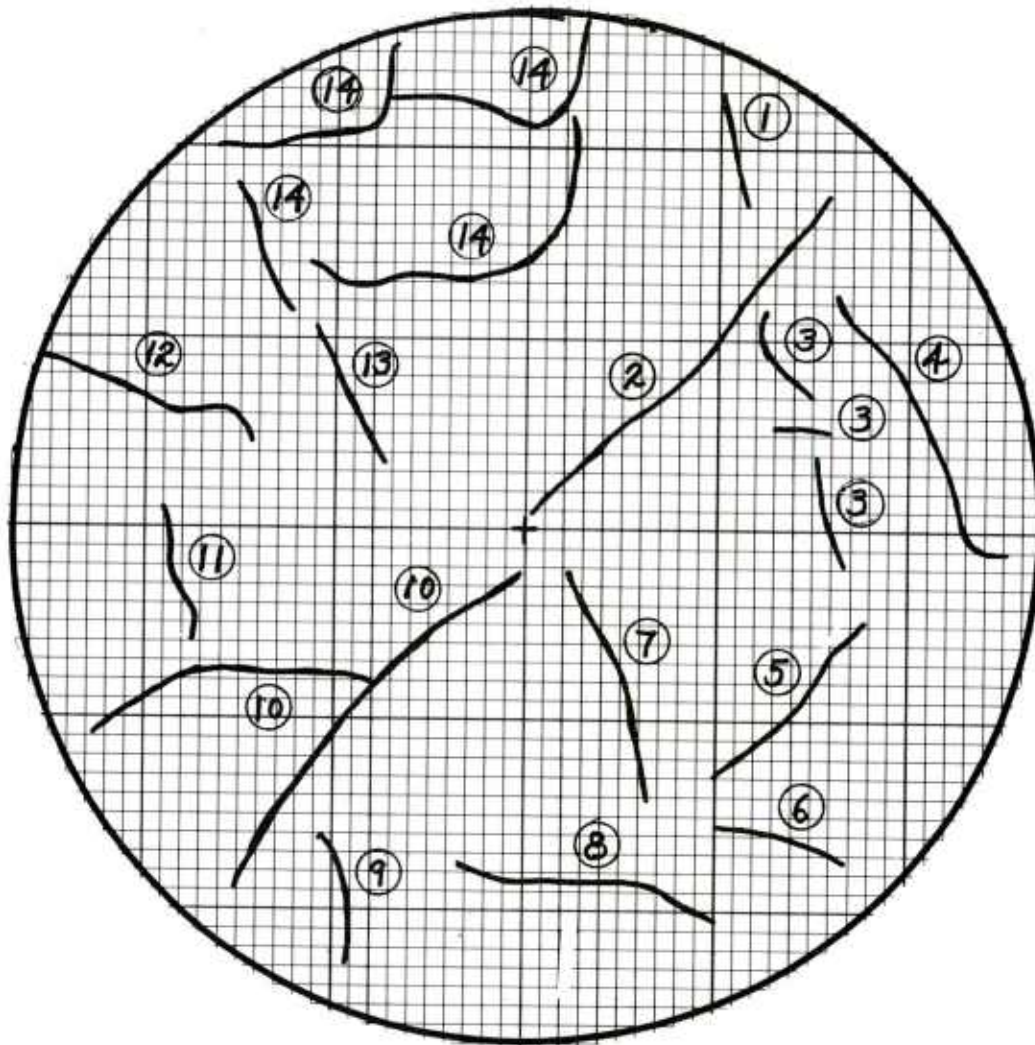


Figure 38. Distribution of cracks in forward surface of M483A1 base CMC/KAAP 61

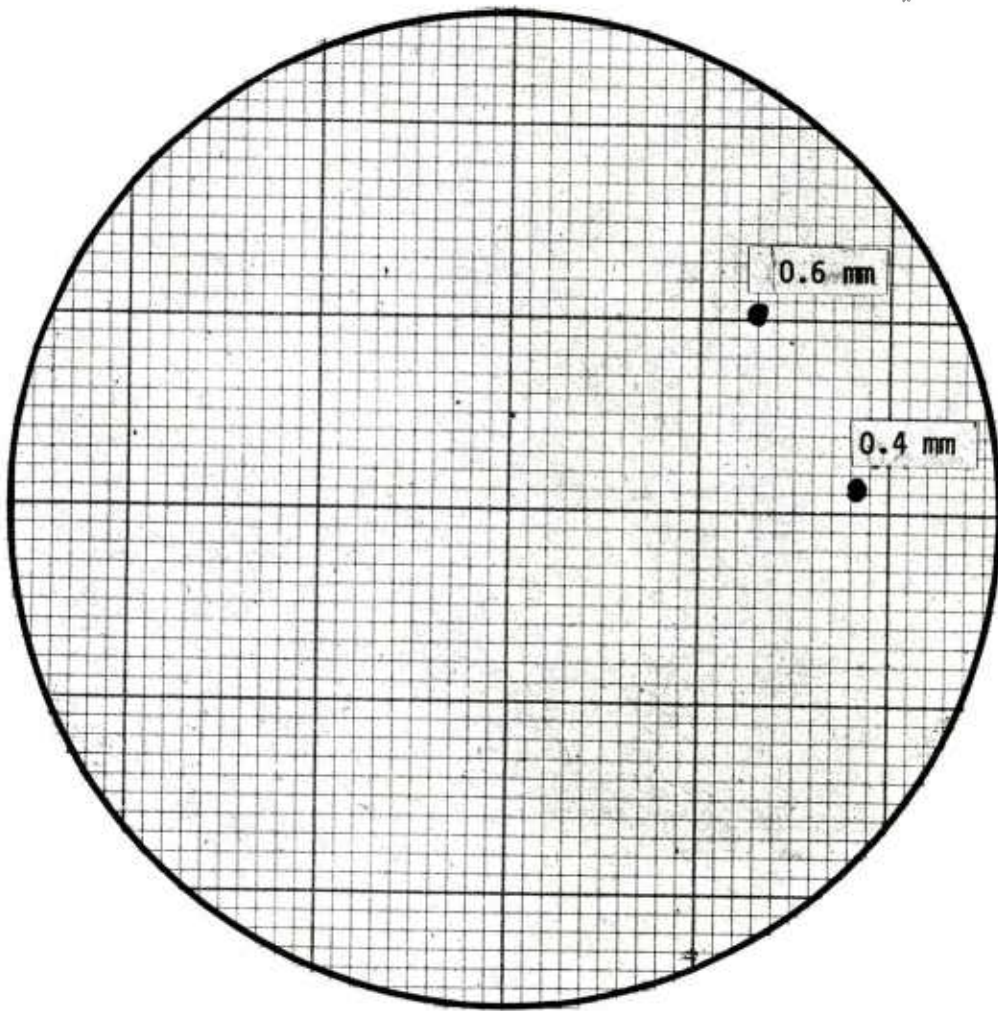


Figure 39. Location and depth of spots on M483A1 base CMC/KAAP 62

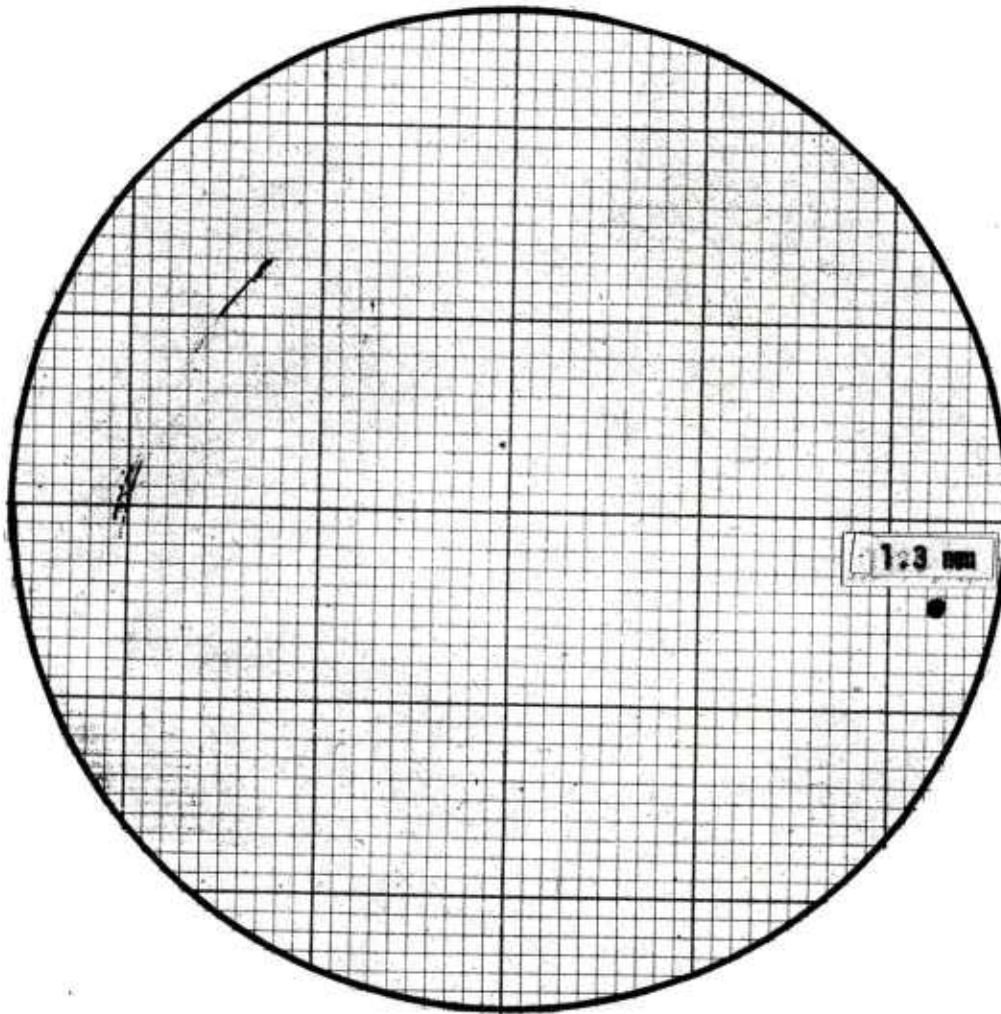


Figure 40. Location and depth of a spot on M483A1 base CMC/KAAP 64

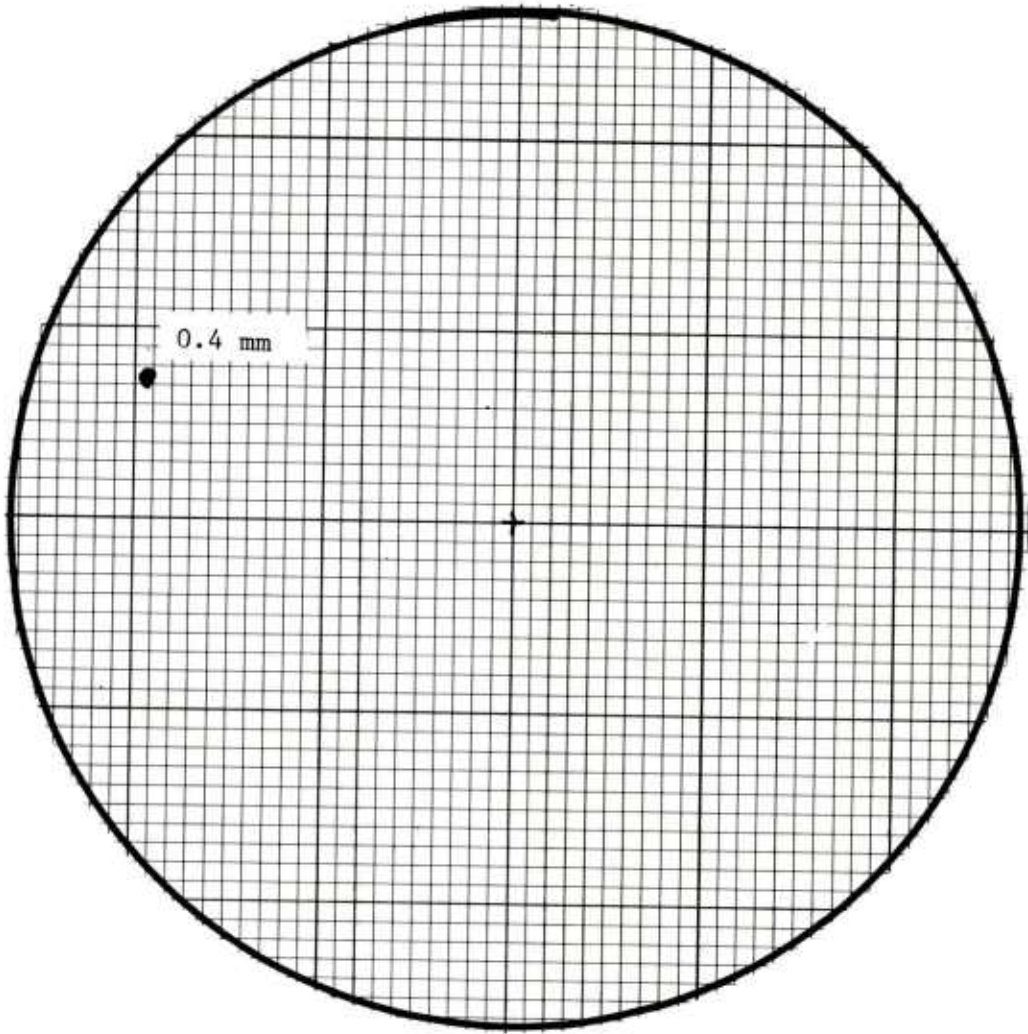


Figure 41. Location and depth of a spot on M483A1 base CMC/KAAP 75

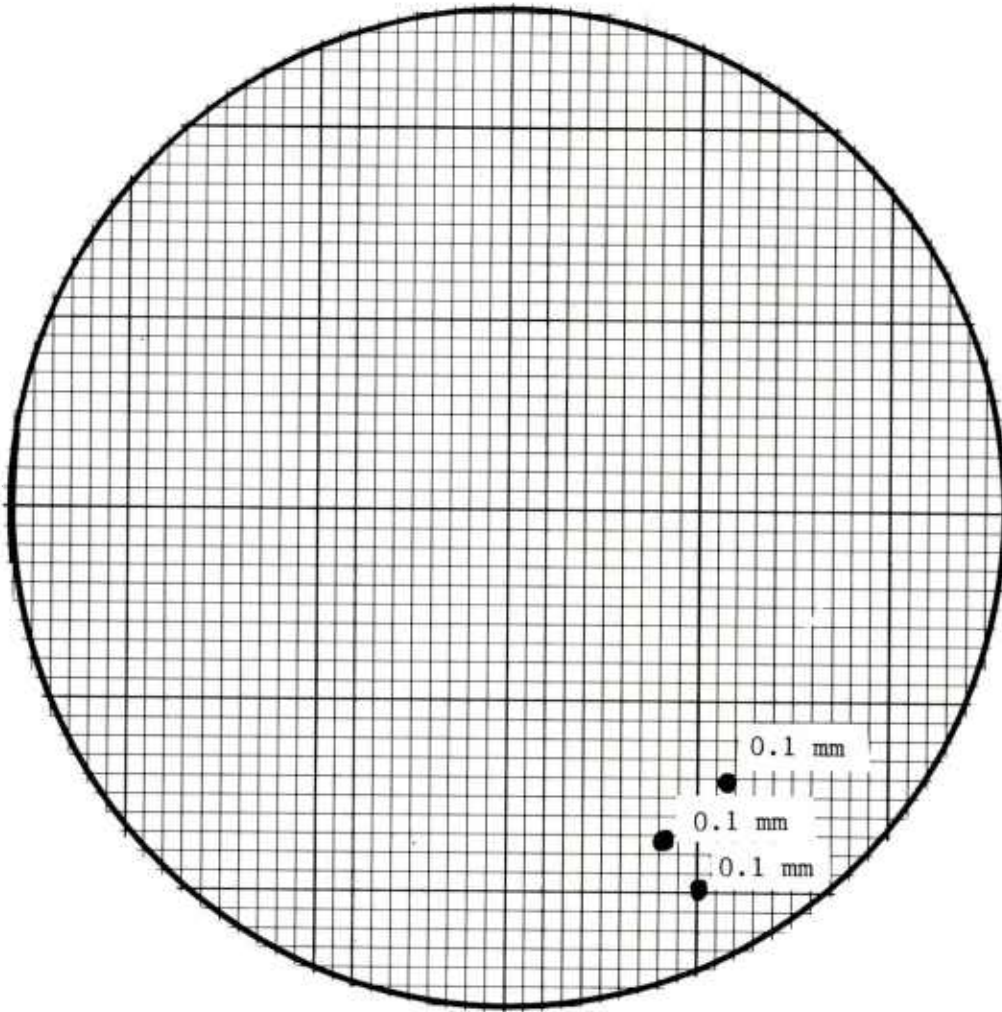


Figure 42. Location and depth of spots on M483A1 base CMC/KAAP 76

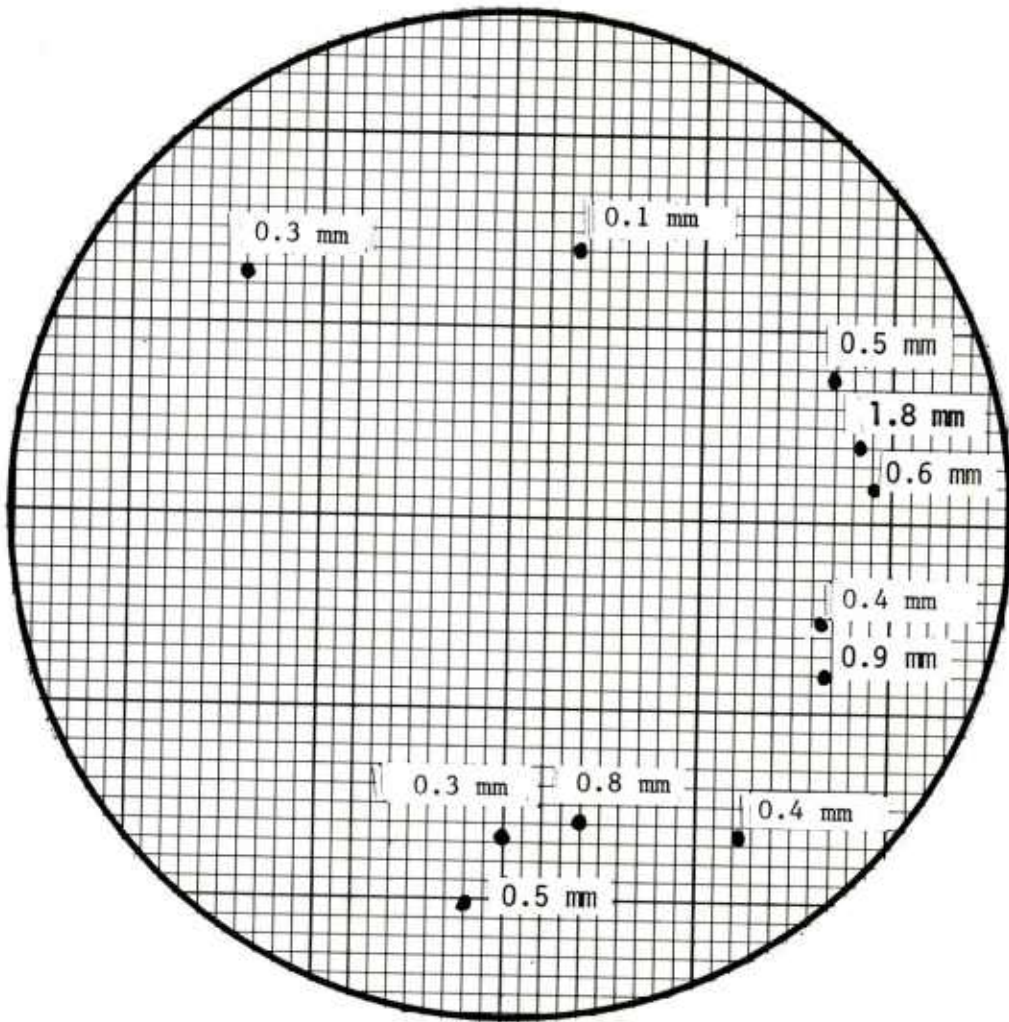


Figure 43. Depth of spots in forward surface of M483A1 base CMC/LSAAP 305



Figure 44. Fluorescent liquid penetrant indications on M692/M731 base  
A-CMC/KAAP 3





Figure 45. Fluorescent liquid penetrant indications on M483Al base CMC/KAAP 61



Figure 46. Fluorescent liquid penetrant indications on M483A1 base CMC/KAAP 71



Figure 47. Fluorescent liquid penetrant indications on M483Al base  
CMC/LSAAP 296

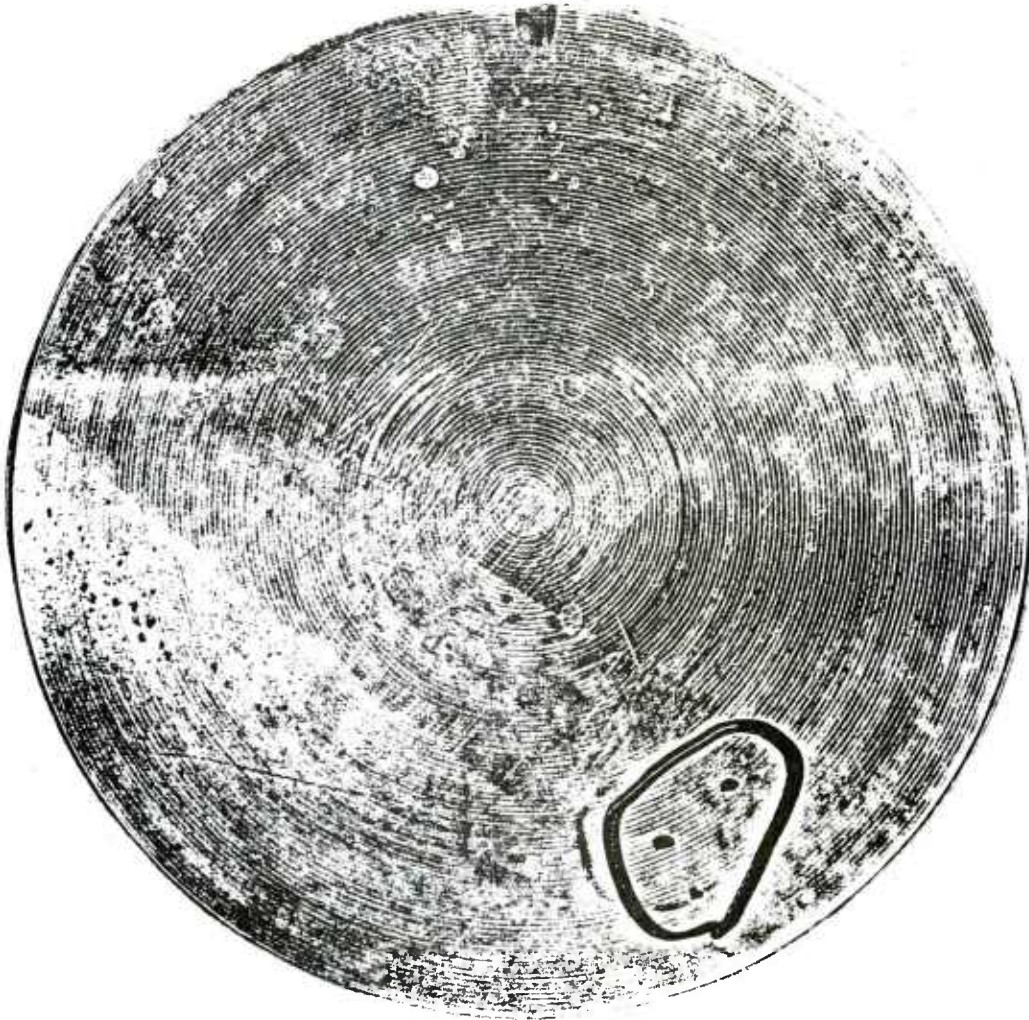


Figure 48. Fluorescent liquid penetrant indications on M483A1 base CMC/KAAP 76

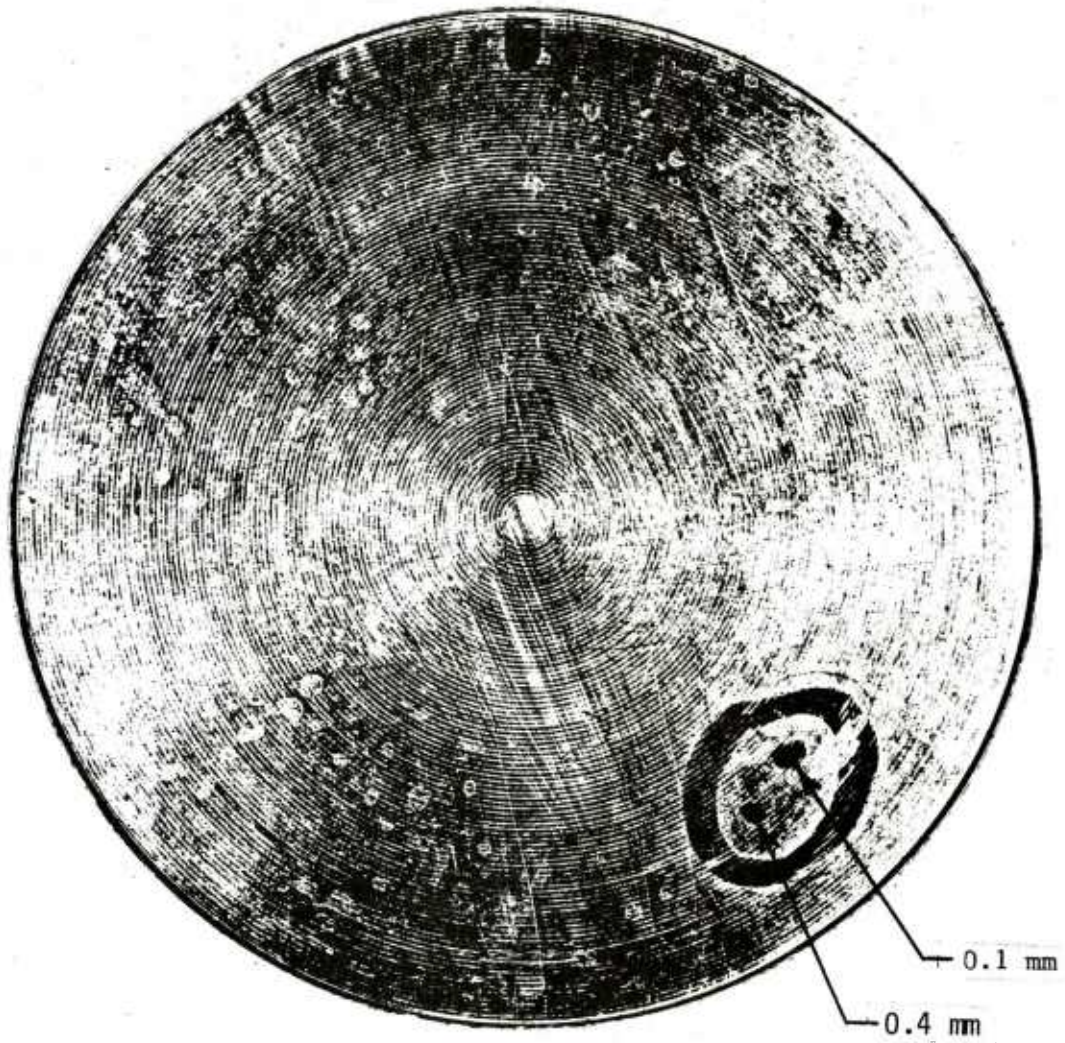


Figure 49. Depth of spots in forward surface of M483A1 base CMC/KAAP 63

DISTRIBUTION LIST

Commander  
U.S. Army Armament Research  
and Development Command

ATTN: DRDAR-QA  
DRDAR-QAS (10)  
DRDAR-QAA  
DRDAR-QAF  
DRDAR-QAC  
DRDAR-QAR  
DRDAR-QAN  
DRDAR-QAM  
DRDAR-LCA  
DRDAR-LCE  
DRDAR-LCM  
DRDAR-LCW  
DRDAR-LCN  
DRDAR-SCP  
DRDAR-SCA  
DRDAR-SCS  
DRDAR-SCM  
DRDAR-TSE  
DRDAR-TSB  
DRDAR-TSS (5)  
DRDAR-TD  
DRDAR-TDS  
DRDAR-TDA  
DRDAR-TDC  
DRDAR-GCL

Dover, NJ 07801

Project Manager  
Cannon Artillery Weapons Systems  
ATTN: DRCPM-CAWS  
Dover, NJ 07801

Project Manager  
Division Air Defense (DIVAD) Gun  
ATTN: DRCPM-ADG  
Dover, NJ 07801

Commander  
U.S. Army Munitions Production  
Base Modernization Agency  
ATTN: SARPM-PBM  
Dover, NJ 07801

Product Manager for  
30mm Ammunition  
ATTN: DRCPM-AAH-30MM  
Dover, NJ 07801

Project Manager  
Tank Main Armament Systems  
ATTN: DRCPM-TMA  
Dover, NJ 07801

Commander  
Aberdeen Proving Ground  
ATTN: STEAP-MT-T, B. 525  
Aberdeen Proving Ground, MD 21005

Commander, Code 33  
Naval Weapons Station  
ATTN: Engineering and Science Div,  
Weapon Quality Engineering Center  
Concord, CA 94520

Commander  
Dahlgren Navy Weapons Laboratory  
ATTN: G53 (Material Science Branch)  
Dahlgren, VA 22448

Director  
U.S. Army Defense Ammunition  
Center and School  
ATTN: SARWR-QA  
Watervliet, NY 12189

Commander  
Foreign Science and Technical Center  
1220 Seventh Street, NE  
ATTN: DRXST-IS3  
Charlottesville, VA 22901

Commander  
Hawthorne Army Ammunition Plant  
DZB Box A  
ATTN: Technical Services  
Babbitt, NV 89416

Commander  
Indiana Army Ammunition Plant  
ATTN: SARIN-QA  
Charlestown, IN 47111

Commander  
U.S. Navy Ordnance Station  
ATTN: Code 40  
Indian Head, MD 20640

Commander  
Iowa Army Ammunition Plant  
ATTN: SARIO-QA  
Middletown, IO 52638

Commander  
Jefferson Proving Ground  
ATTN: STEJP-MTD  
Madison, IN 47250

Commander  
U.S. Army White Sands Missile Range  
ATTN: STEWS-QA-E, B124  
White Sands, NM 88002

Commander  
Kansas Army Ammunition Plant  
ATTN: SARKA-QA  
Parsons, KS 67357

Commander  
Lake City Army Ammunition Plant  
ATTN: SARLC-QA  
E. Independence, MO 64050

Commander  
Lone Star Army Ammunition Plant  
ATTN: SARLS-QA  
Texarkana, TX 75501

Commander  
Longhorn Army Ammunition Plant  
ATTN: SARLO-QA  
Marshall, TX 75670

Commander  
Louisiana Army Ammunition Plant  
ATTN: SARLA-QA  
Shreveport, LA 71130

Commander  
McAlester Army Ammunition Plant  
ATTN: SARMC-QA  
McAlester, OK 74501



Commander  
Milan Army Ammunition Plant  
ATTN: SARMI-QA  
Milan, TN 38358

Commander  
U.S. Navy Research Laboratory  
4555 Overlook Avenue  
ATTN: Code 5835  
Washington, DC 20375

Commander  
U.S. Navy Weapons Center  
ATTN: Code 3682  
China Lake, CA 93555

Commander  
U.S. Navy Weapons Station  
ATTN: Code 40  
Charleston, SC 29408

Commander  
U.S. Navy Weapons Station  
ATTN: Code 401  
Colts Neck, NJ 07722

Commander  
U.S. Navy Weapons Station  
ATTN: Code F321  
Fallbrook, CA 92028

Commander  
U.S. Navy Weapons Station  
ATTN: Code 40  
Yorktown, VA 23691

Commander  
U.S. Navy Weapons Support Center  
ATTN: Code 40  
Crane, IN 47522

Commander  
U.S. Army Pine Bluff Arsenal  
ATTN: SARPB-QA  
Pine Bluff, AR 71602

Commander  
Red River Army Ammunition Plant  
ATTN: SARRR-QA  
Texarkana, TX 75501

Commander  
U.S. Army Armament Materiel  
Readiness Command  
ATTN: DRSAR-LE  
      DRSAR-LEM-M  
      DRSAR-LEP-L  
      DRSAR-QA  
Rock Island, IL 61299

Administrator  
Defense Technical Information Center  
ATTN: Accessions Division (12)  
Cameron Station  
Alexandria, VA 22314

Director  
U.S. Army Materiel Systems  
Analysis Activity  
ATTN: DRXSY-MP  
Aberdeen Proving Ground, MD 21005

Commander/Director  
Chemical Systems Laboratory  
U.S. Army Armament Research  
and Development Command  
ATTN: DRDAR-CLB-PA  
      DRDAR-CLJ-L  
      DRDAR-CLN  
APG, Edgewood Area, MD 21010

Director  
Ballistics Research Laboratory  
U.S. Army Armament Research  
and Development Command  
ATTN: DRDAR-TSB-S  
      DRDAR-BLB  
      DRDAR-BLI  
      DRDAR-BLL  
Aberdeen Proving Ground, MD 21005

Chief  
Benet Weapons Laboratory, LCWSL  
U.S. Army Armament Research  
and Development Command  
ATTN: DRDAR-LCB-TL  
Watervliet, NY 12189

Director  
U.S. Army TRADOC Systems  
Analysis Activity  
ATTN: ATAA-SL  
White Sands Missile Range, NM 88002

Commander  
U.S. Army Research and  
Technology Laboratories  
ATTN: DAVDL-EU  
Ft. Eustis, VA 23604

Director  
U.S. Army Research and  
Technology Laboratories  
AMES Research Center  
ATTN: DAVDL-AS  
Moffett Field, CA 94035

Director  
U.S. Defense Ammunition Center and School  
ATTN: SARAC-DEN  
Savanna, IL 61074